Supporting Information

RSC Advances

Solvent-polarity reconfigurable fluorescent 4-piperazino-*N*-aryl-1,8-naphthalimide crown ether logic gates

Gabriel Gauci and David C. Magri*

Department of Chemistry, Faculty of Science
University of Malta, Msida, Malta, MSD 2080
email: david.magri@um.edu.mt
Phone: (+356) 2340 2276

Table of Contents

1. Experimental

All reagents were purchased from commercial suppliers and used without further purification: 4'-aminobenzo-18-crown-6 (98%, Fluka), 4'-aminobenzo-15-crown-5 (97%, Sigma-Aldrich), 3,4-dimethoxyaniline (>98%, TCI), aniline (GPR, BDH), 4-chloro-1,8-naphthalic anhydride (94%, Alfa Aesar), piperazine (>99%, Sigma Aldrich), hydrochloric acid (37 %, Sigma Aldrich), tetramethylammonium hydroxide (25 % (*w/w*) in water, Sigma Aldrich), chloroform-*d* (99.8 atom % D with 0.03% TMS, Sigma Aldrich), deuterium oxide (99.9 atom % D, Sigma Aldrich), methanol-d_4 (99.8 atom % D with 0.03% TMS, Sigma Aldrich). HPLC grade solvents were purchased from Carlo Erba. The 4-chloro-*N*-aryl-1,8-naphthalimide intermediates were synthesised according to our previous work.[1] Metal cations were used as the chloride salts.

NMR spectra were acquired with a Bruker Avance III HD NMR spectrometer fitted with an Ascend 500 11.75 Tesla superconducting magnet and a multinuclear 5mm PABBO probe. The frequencies are 500.13 MHz for ^{1}H-NMR and 125.76 MHz for ^{13}C-NMR, respectively. Data were analysed and processed with Topspin version 4.0.5. Chemical shifts were reported in ppm downfield with respect to TMS at 0.00 ppm at 298 K. Data for ^{1}H-NMR is reported with multiplicity (s = singlet, d = doublet, t = triplet, m = multiplet). Infrared spectra were recorded using a Shimadzu IR-Affinity-1 spectrophotometer between 4000-500 cm^{-1}. High resolution mass spectrometry (HRMS) was performed by ESI-ToF outsourced to Medac Ltd. (UK). http://medacltd.com/

Ultraviolet-visible absorption spectroscopy data was obtained with a dual beamed Jasco V-650 spectrophotometer and processed with Spectra Manager V.2.0. Spectra were recorded at 1 nm data intervals and a scan rate of 400 nm/min. The fluorescence spectra were acquired with a Jasco FP-8300 spectrophotometer and processed with the same version of Spectra Manager. Quartz SUPRASIL cuvettes (101-10-40) with 10 mm pathlength with transparent windows on all four sides were used. The excitation wavelengths were the absorbance maxima. The parameters for the data acquisition were data intervals of 0.2 nm, excitation bandwidth of 2.5 nm, emission bandwidth of 2.5 nm, scan rate of 500 nm/min and a sensitivity response set to high. The pH was monitored using a HANNA pH 210 Microprocessor pH meter. The pH meter was calibrated with buffer solutions of pH 7.0 and pH 4.0.

The quantum yields of **1-4** in various solvents were determined via the relative determination method, using quinine hemisulfate monohydrate in 0.1 M sulfuric acid as the reference compound (ϕ_{ref} = 0.546).

$$\phi_{smp} = \phi_{ref}\, x \frac{I_{smp}}{I_{ref}} x \frac{A_{ref}}{A_{smp}} x \frac{n_{smp}^2}{n_{ref}^2}$$

where ϕ_{smp} is the relative fluorescence quantum yield of the sample, ϕ_{ref} is the fluorescence quantum yield of the reference standard, I_{smp} is the emission area of the sample, I_{ref} is the emission area of the reference standard, A_{ref} is the absorbance of the reference standard, A_{smp} is the absorbance of the sample, n_{smp} is the solvent refractive index of the sample, and n_{std} is the solvent refractive index of the reference standard.

References

1. A. Diacono, M. C. Aquilina, A. Calleja, G. Agius, G. Gauci, K. Szaciłowski, and D. C. Magri, *Org. Biomol. Chem.*, 2020, **18**, 4773.

2. Characterisation data of 1-4
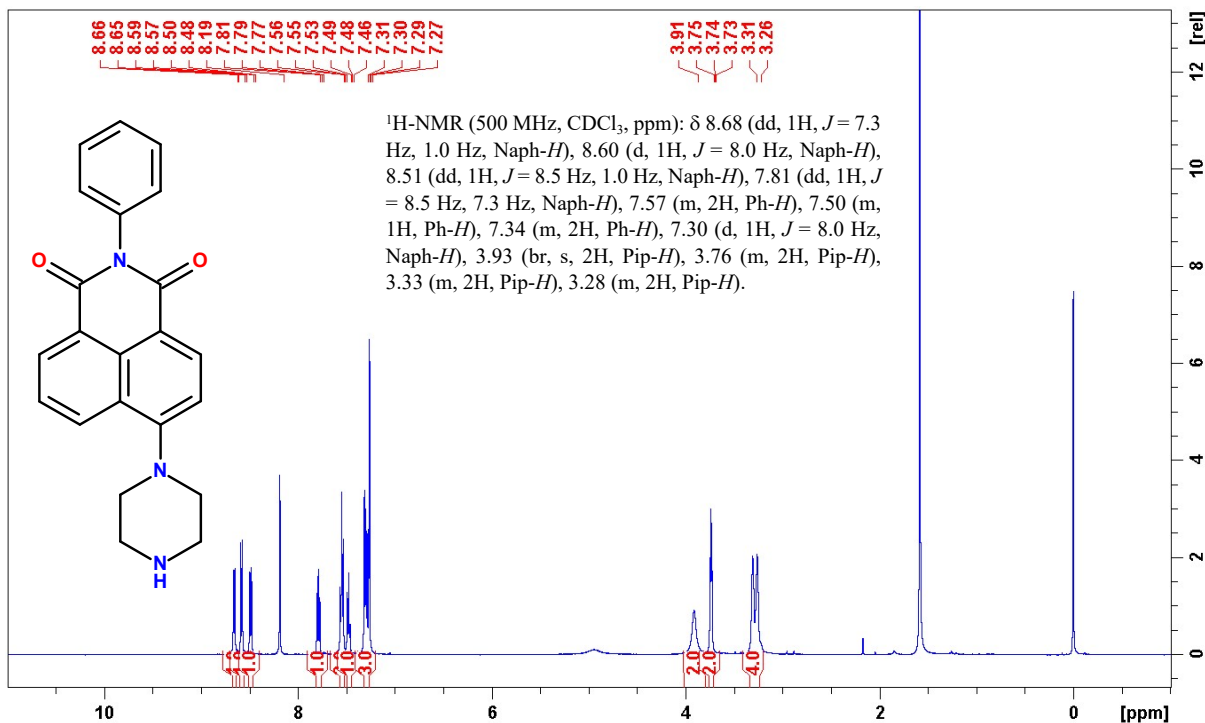
2.1. ^{1}H NMR spectra of 1-4

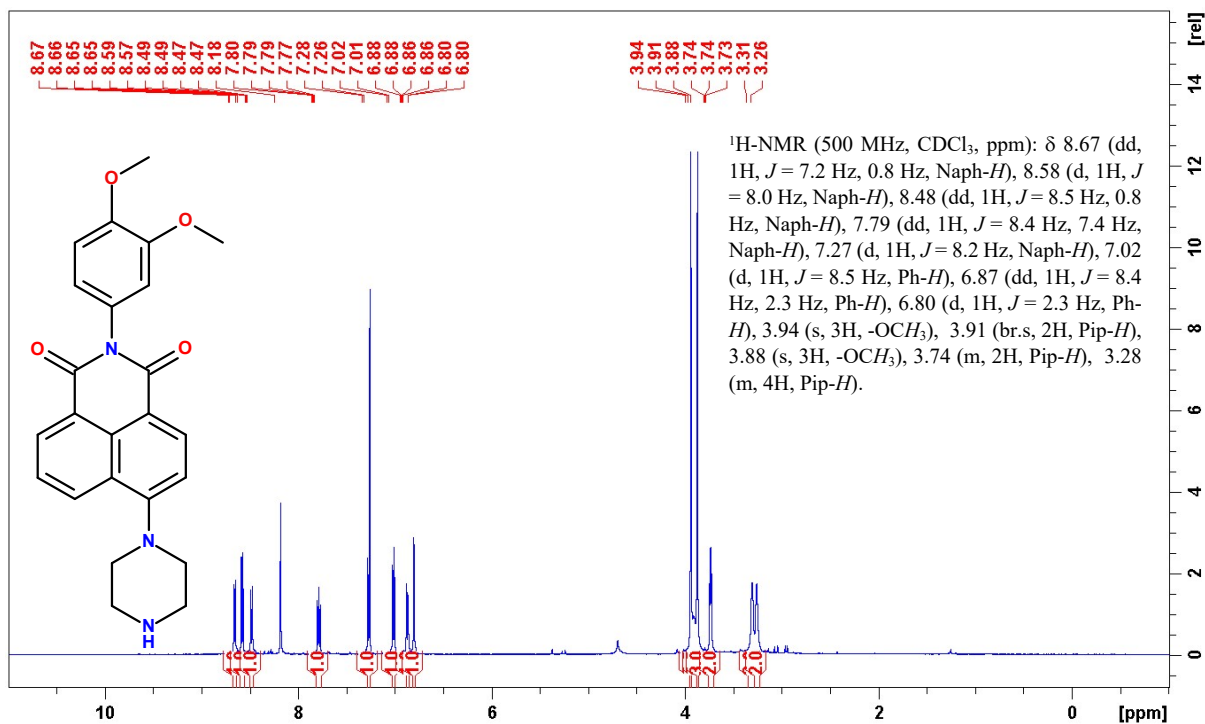**Figure S1.** ^{1}H NMR spectrum of 4-piperazino-*N*-phenyl-1,8-naphthalimide **1** in CDCl$_3$ (with 0.03% TMS).

The NMR annotation in Figure S1 reads:

^{1}H-NMR (500 MHz, CDCl$_3$, ppm): δ 8.68 (dd, 1H, *J* = 7.3 Hz, 1.0 Hz, Naph-*H*), 8.60 (d, 1H, *J* = 8.0 Hz, Naph-*H*), 8.51 (dd, 1H, *J* = 8.5 Hz, 1.0 Hz, Naph-*H*), 7.81 (dd, 1H, *J* = 8.5 Hz, 7.3 Hz, Naph-*H*), 7.57 (m, 2H, Ph-*H*), 7.50 (m, 1H, Ph-*H*), 7.34 (m, 2H, Ph-*H*), 7.30 (d, 1H, *J* = 8.0 Hz, Naph-*H*), 3.93 (br, s, 2H, Pip-*H*), 3.76 (m, 2H, Pip-*H*), 3.33 (m, 2H, Pip-*H*), 3.28 (m, 2H, Pip-*H*).

Figure S2. ^{1}H NMR spectrum of 4-piperazino-*N*-(3,4-dimethoxyphenyl)-1,8-naphthalimide **2** in CDCl$_3$.

The NMR annotation in Figure S2 reads:

^{1}H-NMR (500 MHz, CDCl$_3$, ppm): δ 8.67 (dd, 1H, *J* = 7.2 Hz, 0.8 Hz, Naph-*H*), 8.58 (d, 1H, *J* = 8.0 Hz, Naph-*H*), 8.48 (dd, 1H, *J* = 8.5 Hz, 0.8 Hz, Naph-*H*), 7.79 (dd, 1H, *J* = 8.4 Hz, 7.4 Hz, Naph-*H*), 7.27 (d, 1H, *J* = 8.2 Hz, Naph-*H*), 7.02 (d, 1H, *J* = 8.5 Hz, Ph-*H*), 6.87 (dd, 1H, *J* = 8.4 Hz, 2.3 Hz, Ph-*H*), 6.80 (d, 1H, *J* = 2.3 Hz, Ph-*H*), 3.94 (s, 3H, -OC*H*$_3$), 3.91 (br.s, 2H, Pip-*H*), 3.88 (s, 3H, -OC*H*$_3$), 3.74 (m, 2H, Pip-*H*), 3.28 (m, 4H, Pip-*H*).
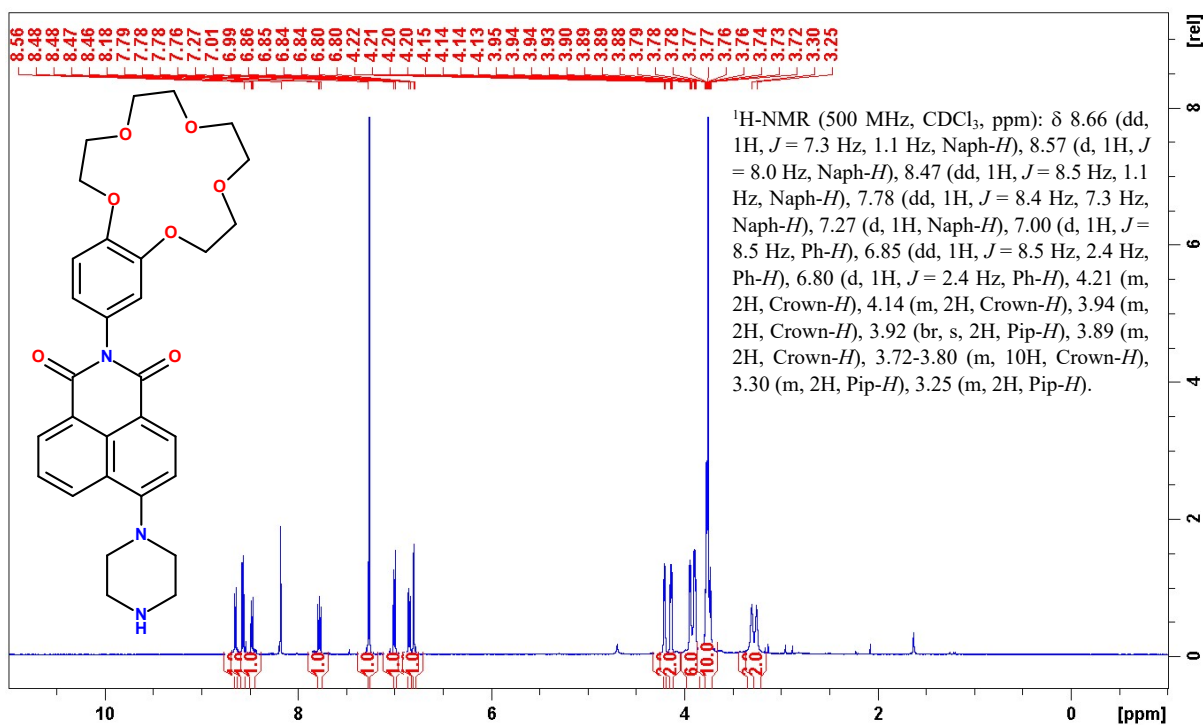
Figure S3. ^{1}H NMR spectrum of 4-piperazino-*N*-(benzo-15-crown-5)-1,8-naphthalimide **3** in CDCl$_3$.

^{1}H-NMR (500 MHz, CDCl$_3$, ppm): δ 8.66 (dd, 1H, *J* = 7.3 Hz, 1.1 Hz, Naph-*H*), 8.57 (d, 1H, *J* = 8.0 Hz, Naph-*H*), 8.47 (dd, 1H, *J* = 8.5 Hz, 1.1 Hz, Naph-*H*), 7.78 (dd, 1H, *J* = 8.4 Hz, 7.3 Hz, Naph-*H*), 7.27 (d, 1H, Naph-*H*), 7.00 (d, 1H, *J* = 8.5 Hz, Ph-*H*), 6.85 (dd, 1H, *J* = 8.5 Hz, 2.4 Hz, Ph-*H*), 6.80 (d, 1H, *J* = 2.4 Hz, Ph-*H*), 4.21 (m, 2H, Crown-*H*), 4.14 (m, 2H, Crown-*H*), 3.94 (m, 2H, Crown-*H*), 3.92 (br, s, 2H, Pip-*H*), 3.89 (m, 2H, Crown-*H*), 3.72-3.80 (m, 10H, Crown-*H*), 3.30 (m, 2H, Pip-*H*), 3.25 (m, 2H, Pip-*H*).
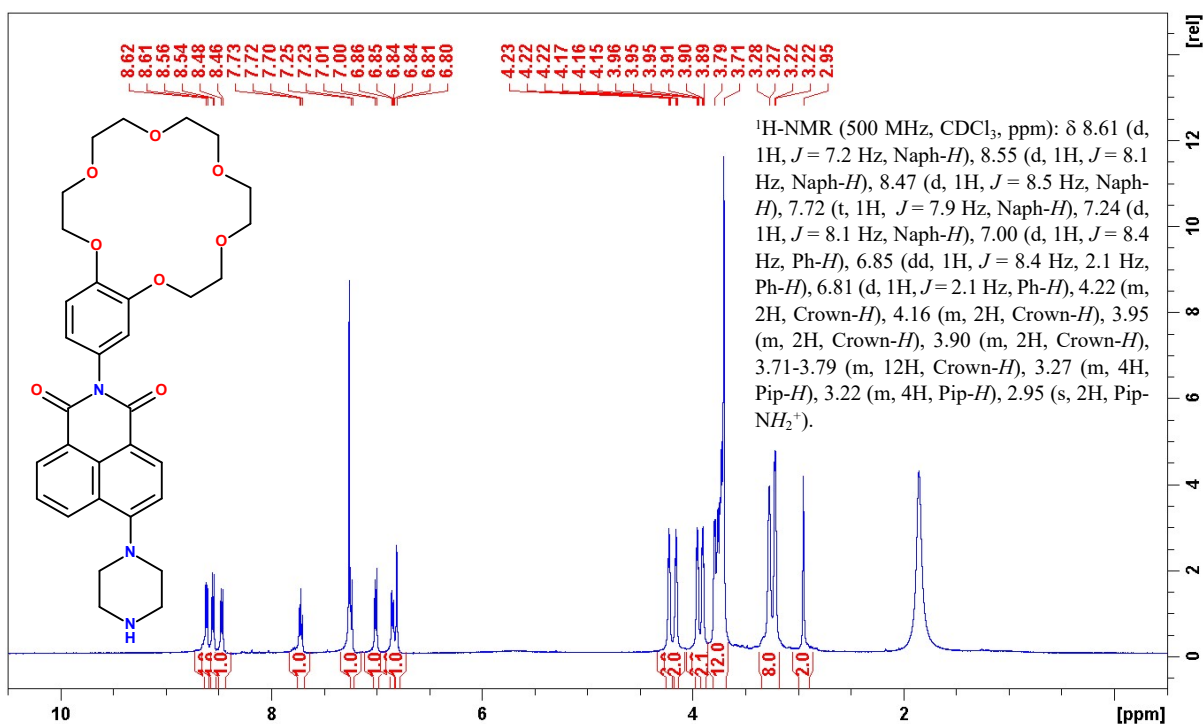
Figure S4. ^{1}H NMR spectrum of 4-piperazino-*N*-(benzo-18-crown-6)-1,8-naphthalimide **4** in CDCl$_3$.

^{1}H-NMR (500 MHz, CDCl$_3$, ppm): δ 8.61 (d, 1H, *J* = 7.2 Hz, Naph-*H*), 8.55 (d, 1H, *J* = 8.1 Hz, Naph-*H*), 8.47 (d, 1H, *J* = 8.5 Hz, Naph-*H*), 7.72 (t, 1H, *J* = 7.9 Hz, Naph-*H*), 7.24 (d, 1H, *J* = 8.1 Hz, Naph-*H*), 7.00 (d, 1H, *J* = 8.4 Hz, Ph-*H*), 6.85 (dd, 1H, *J* = 8.4 Hz, 2.1 Hz, Ph-*H*), 6.81 (d, 1H, *J* = 2.1 Hz, Ph-*H*), 4.22 (m, 2H, Crown-*H*), 4.16 (m, 2H, Crown-*H*), 3.95 (m, 2H, Crown-*H*), 3.90 (m, 2H, Crown-*H*), 3.71-3.79 (m, 12H, Crown-*H*), 3.27 (m, 4H, Pip-*H*), 3.22 (m, 4H, Pip-*H*), 2.95 (s, 2H, Pip-N*H$_2$*$^+$).

2.2. ^{13}C and ^{13}C DEPT-135 NMR spectra of 1-4

^{13}C-NMR (125 MHz, CDCl$_3$, ppm): δ 40.21 (CH$_2$), 45.77 (CH$_2$), 52.72 (CH$_2$), 53.53 (CH$_2$), 115.73 (CH), 117.95 (C), 123.60 (C), 126.35 (C), 126.50 (CH), 128.70 (2CH), 129.36 (2CH), 129.97 (CH), 130.24 (C), 131.72 (CH), 132.75 (CH), 135.49 (C), 155.27 (C), 164.00 (CO), 164.48 (CO).
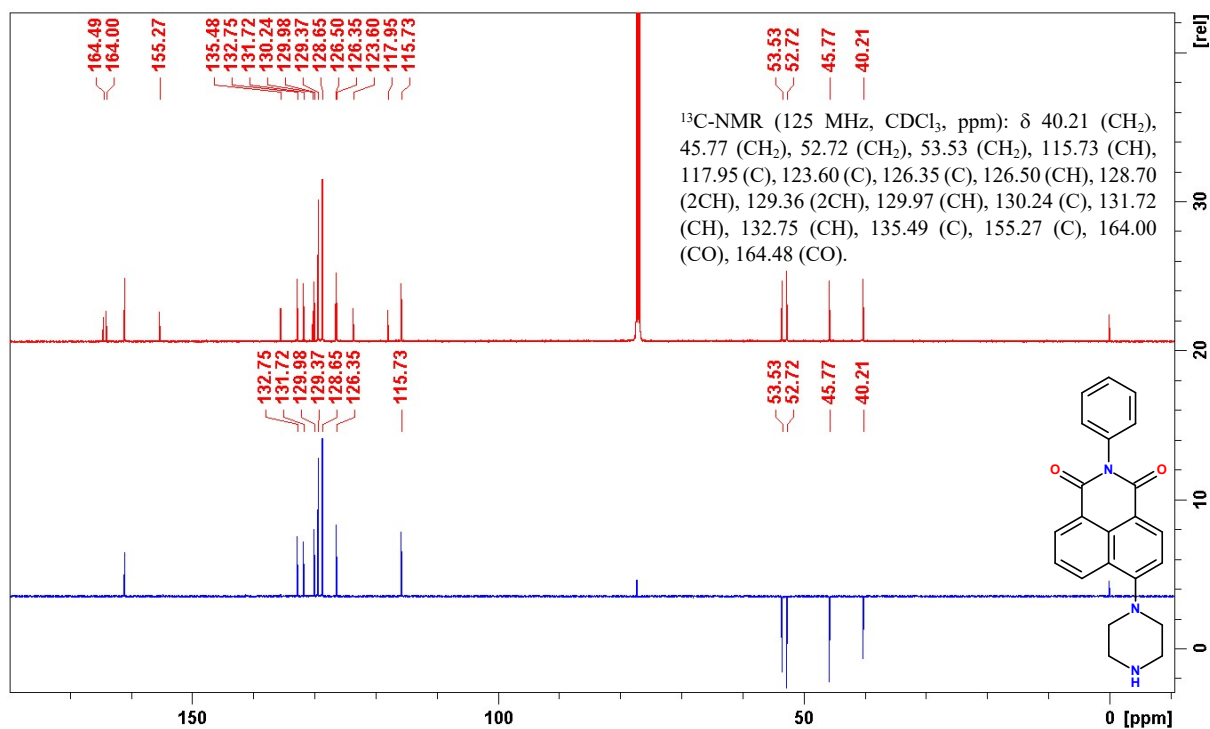
Figure S5. ^{13}C NMR (top) and ^{13}C DEPT-135 (bottom) spectra of 4-piperazino-*N*-phenyl-1,8-naphthalimide **1** in CDCl$_3$ (with 0.03% TMS).

^{13}C-NMR (125 MHz, CDCl$_3$, ppm): δ 40.21 (CH$_2$), 45.77 (CH$_2$), 52.73 (CH$_2$), 53.52 (CH$_2$), 55.94 (-OCH$_3$), 56.05 (-OCH$_3$), 111.42 (CH), 111.78 (CH), 115.72 (CH), 117.95 (C), 120.76 (CH), 123.61 (C), 126.35 (CH), 128.16 (C), 129.98 (CH), 130.20 (C), 131.75 (CH), 132.78 (CH), 149.17 (C), 149.61 (C), 155.26 (C), 164.23 (CO), 164.71 (CO).
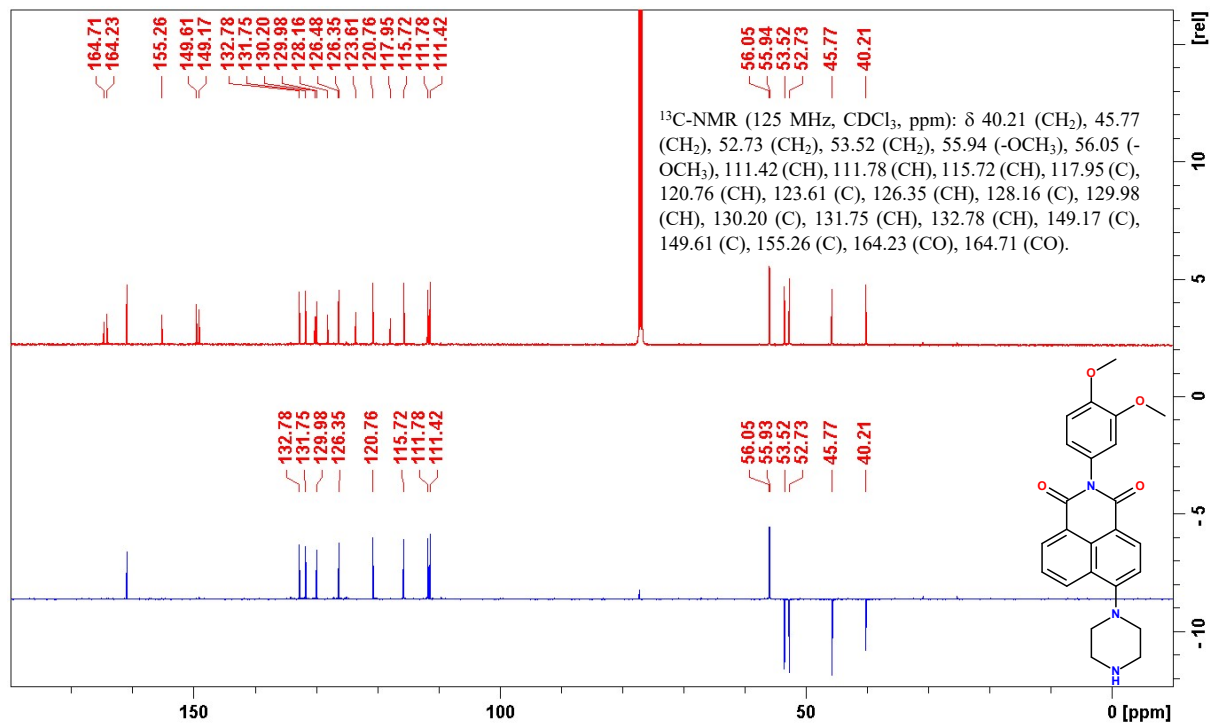
Figure S6. ^{13}C NMR (top) and ^{13}C DEPT-135 (bottom) spectra of 4-piperazino-*N*-(3,4-dimethoxyphenyl)-1,8-naphthalimide **2** in CDCl$_3$.
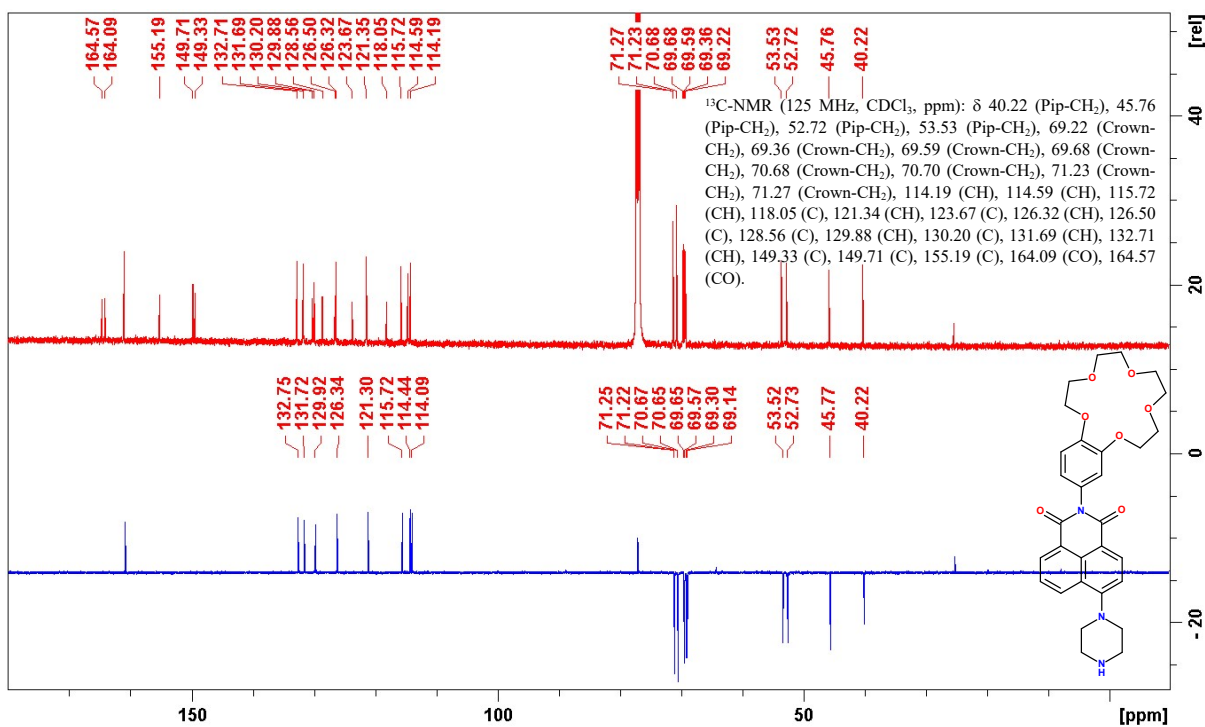
Figure S7. ^{13}C NMR (top) and ^{13}C DEPT-135 (bottom) spectra of 4-piperazino-*N*-(benzo-15-crown-5)-1,8-naphthalimide **3** in CDCl$_3$.

^{13}C-NMR (125 MHz, CDCl$_3$, ppm): δ 40.22 (Pip-CH$_2$), 45.76 (Pip-CH$_2$), 52.72 (Pip-CH$_2$), 53.53 (Pip-CH$_2$), 69.22 (Crown-CH$_2$), 69.36 (Crown-CH$_2$), 69.59 (Crown-CH$_2$), 69.68 (Crown-CH$_2$), 70.68 (Crown-CH$_2$), 70.70 (Crown-CH$_2$), 71.23 (Crown-CH$_2$), 71.27 (Crown-CH$_2$), 114.19 (CH), 114.59 (CH), 115.72 (CH), 118.05 (C), 121.34 (CH), 123.67 (C), 126.32 (CH), 126.50 (C), 128.56 (C), 129.88 (CH), 130.20 (C), 131.69 (CH), 132.71 (CH), 149.33 (C), 149.71 (C), 155.19 (C), 164.09 (CO), 164.57 (CO).
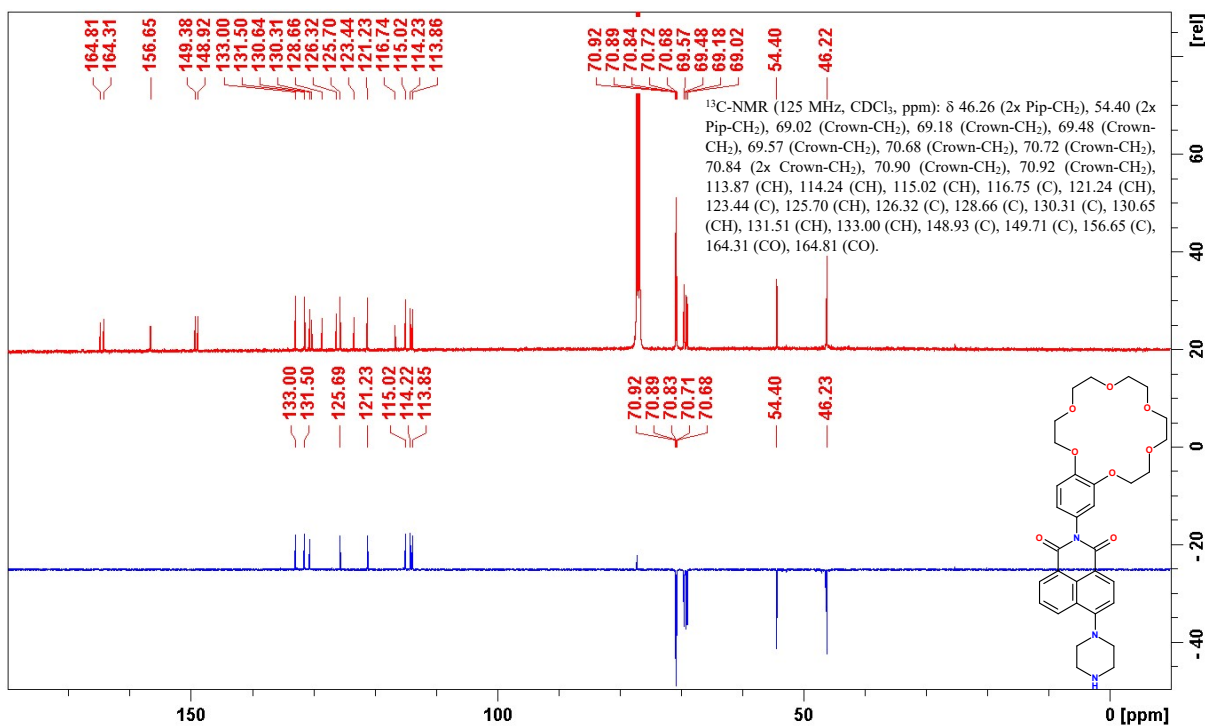
Figure S8. ^{13}C NMR (top) and ^{13}C DEPT-135 (bottom) spectra of 4-piperazino-*N*-(benzo-18-crown-6)-1,8-naphthalimide **4** in CDCl$_3$.

^{13}C-NMR (125 MHz, CDCl$_3$, ppm): δ 46.26 (2x Pip-CH$_2$), 54.40 (2x Pip-CH$_2$), 69.02 (Crown-CH$_2$), 69.18 (Crown-CH$_2$), 69.48 (Crown-CH$_2$), 69.57 (Crown-CH$_2$), 70.68 (Crown-CH$_2$), 70.72 (Crown-CH$_2$), 70.84 (2x Crown-CH$_2$), 70.90 (Crown-CH$_2$), 70.92 (Crown-CH$_2$), 113.87 (CH), 114.24 (CH), 115.02 (CH), 116.75 (C), 121.24 (CH), 123.44 (C), 125.70 (CH), 126.32 (C), 128.66 (C), 130.31 (C), 130.65 (CH), 131.51 (CH), 133.00 (CH), 148.93 (C), 149.71 (C), 156.65 (C), 164.31 (CO), 164.81 (CO).

2.3. HRMS spectra of 1-4

HRMS (ES-TOF, m/z): calculated $C_{22}H_{20}N_3O_2$ 358.1556, found 358.1550.
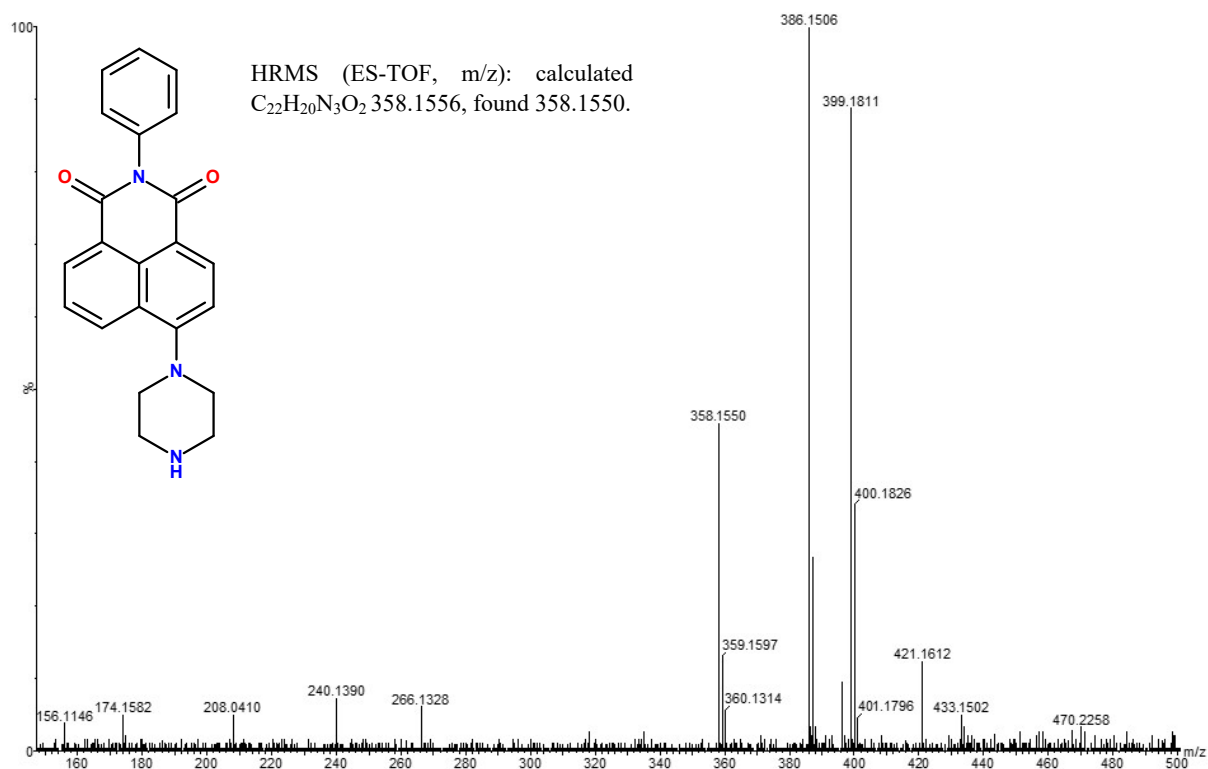
Figure S9. HRMS spectrum of 4-piperazino-*N*-phenyl-1,8-naphthalimide **1**.

HRMS (ES-TOF, m/z): calculated $C_{22}H_{20}N_3O_2$ 418.1752, found 418.1767.
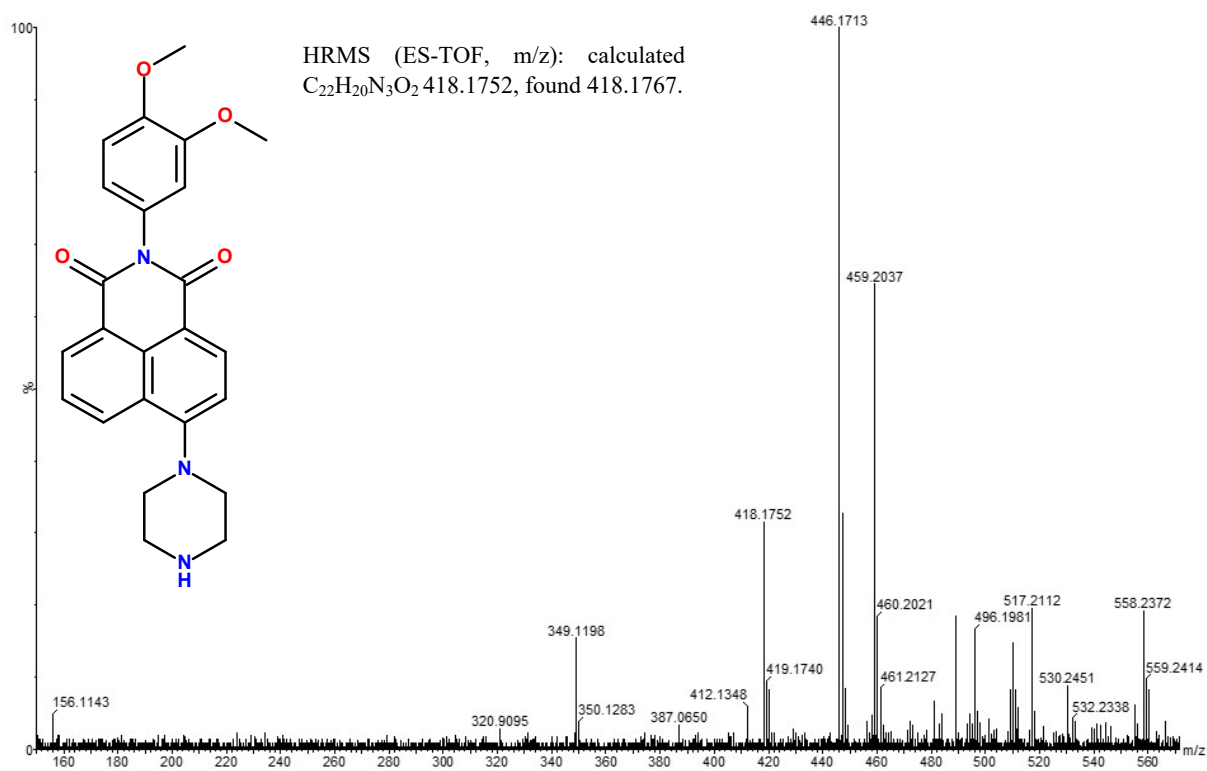
Figure S10. HRMS spectrum of 4-piperazino-*N*-(3,4-dimethoxyphenyl)-1,8-naphthalimide **2**.

HRMS (ES-TOF, m/z): calculated $C_{30}H_{34}N_3O_7$ 548.2397, found 548.2379.
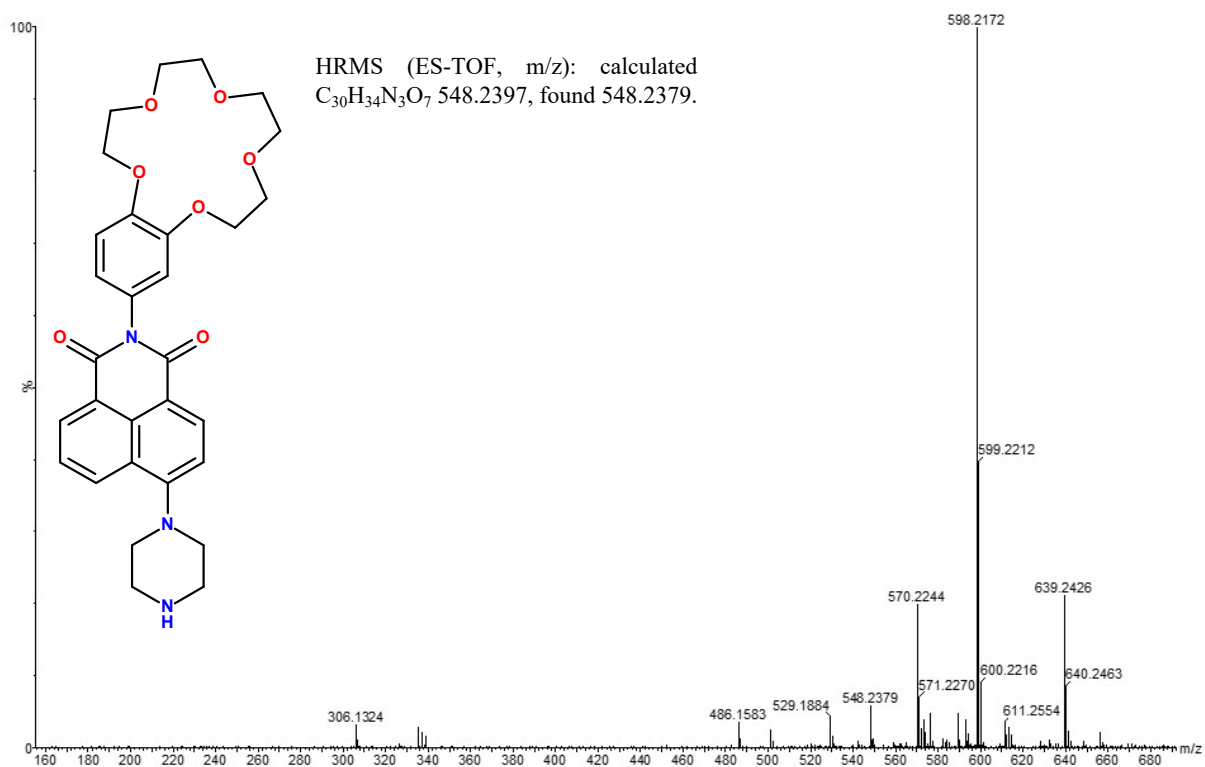
Figure S11. HRMS spectrum of 4-piperazino-*N*-(benzo-15-crown-5)-1,8-naphthalimide **3**.

HRMS (ES-TOF, m/z): calculated $C_{32}H_{38}N_3O_8$ 592.2653, found 592.2657.
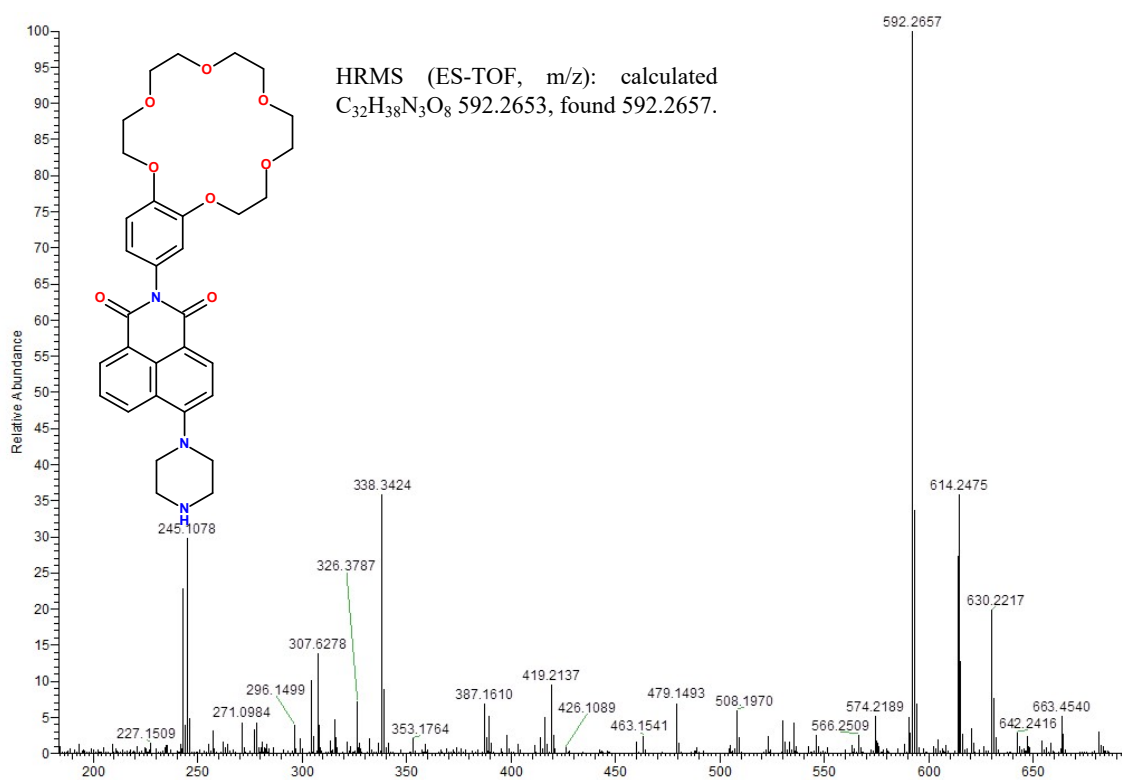
Figure S12. HRMS spectrum of 4-piperazino-*N*-(benzo-18-crown-6)-1,8-naphthalimide **4**.

2.4. IR spectra of 1-4.

IR v_{max} (NaCl, cm^{-1}):
3064, 2906, 2831, 1699,
1653, 1560, 1507, 1369,
1232, 1004, 787, 740.
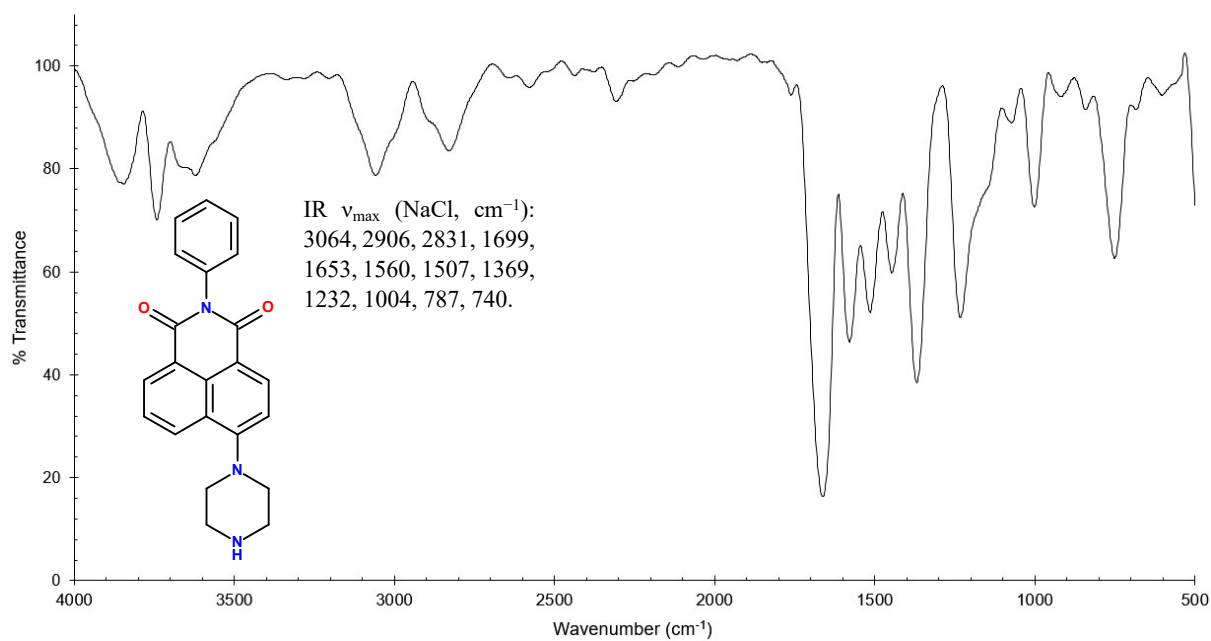
Figure S13. IR spectrum of 4-piperazino-*N*-phenyl-1,8-naphthalimide **1** (thin film on NaCl disk).

IR v_{max} (NaCl, cm^{-1}):
3008, 2929, 2835, 1705,
1662, 1585, 1512, 1436,
1369, 1238, 1002, 754.
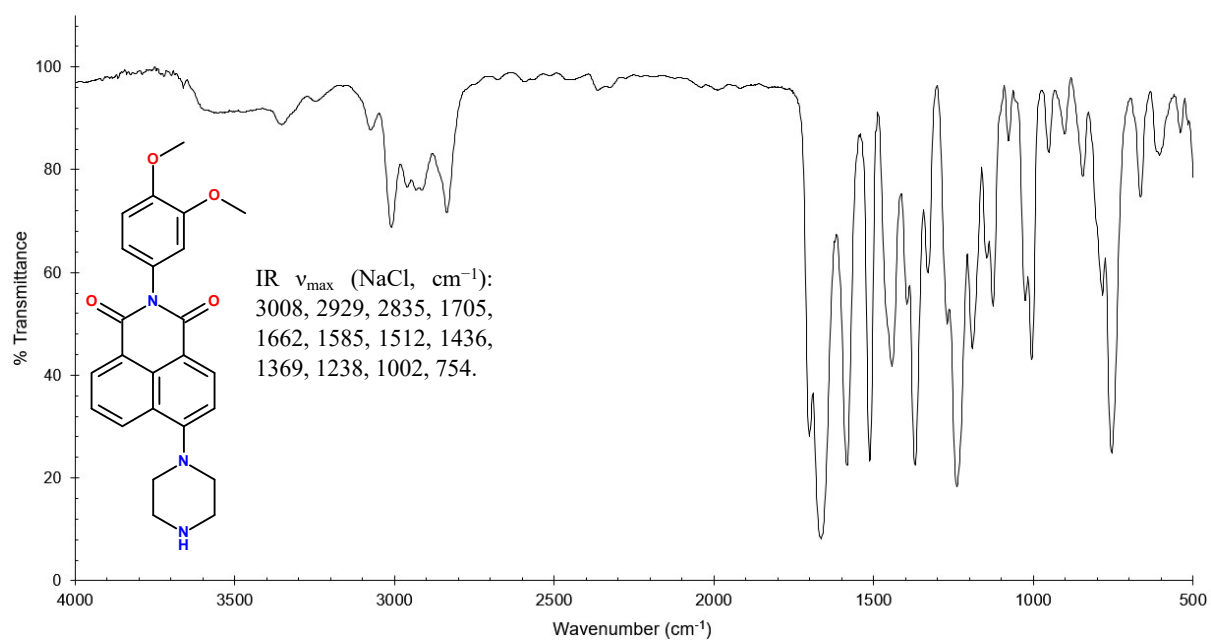
Figure S14. IR spectrum of 4-piperazino-*N*-(3,4-dimethoxyphenyl)-1,8-naphthalimide **2** (thin film on NaCl disk).

IR ν_{max} (NaCl, cm^{-1}):
3064, 2920, 2864, 1683,
1654, 1506, 1456, 1375,
1238, 1122, 1002, 771.
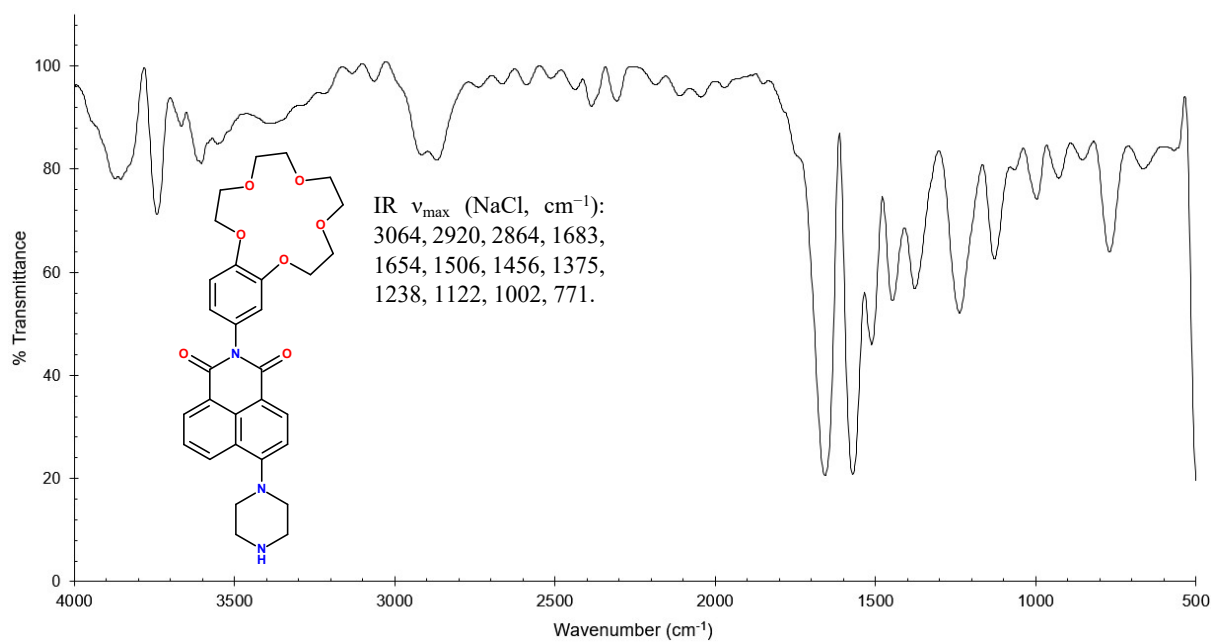
Figure S15. IR spectrum of 4-piperazino-*N*-(benzo-15-crown-5)-1,8-naphthalimide **3** (thin film on NaCl disk).

IR ν_{max} (NaCl, cm^{-1}):
3064, 2914, 1695, 1652,
1585, 1506, 1456, 1375,
1247, 1122, 945, 756.
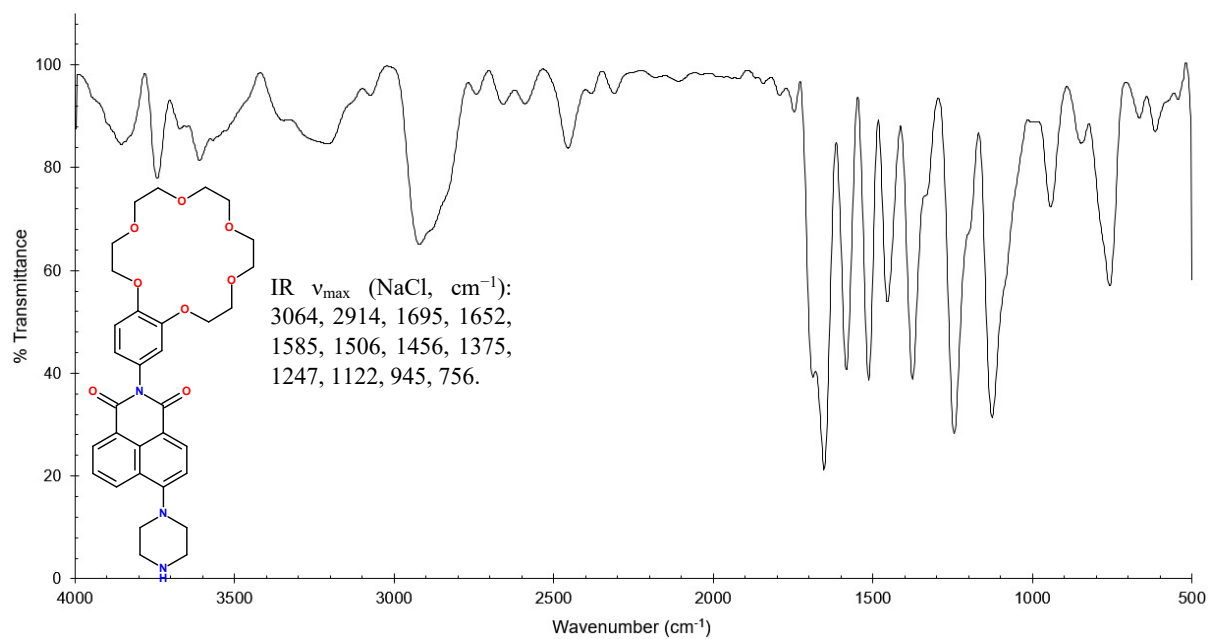
Figure S16. IR spectrum of 4-piperazino-*N*-(benzo-18-crown-6)-1,8-naphthalimide **4** (thin film on NaCl disk).

3. UV-vis absorption and fluorescence emission spectra for 1-4

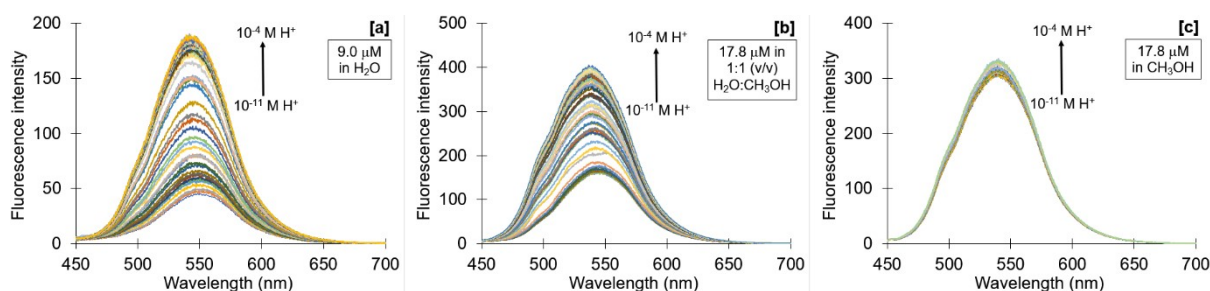## 3.1. Proton UV-vis absorption spectra for 1-4
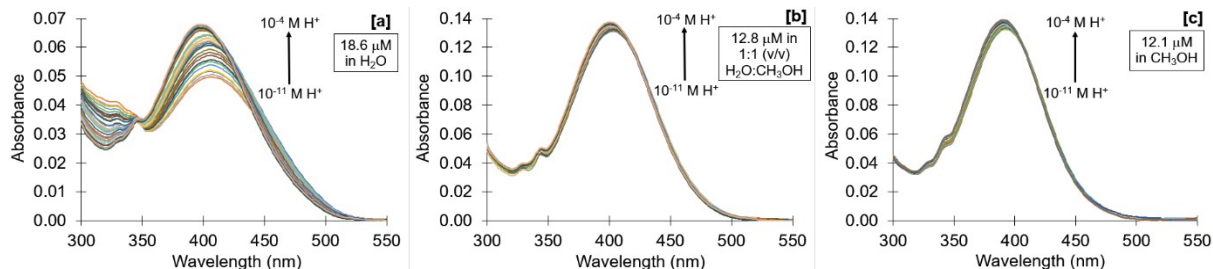
Figure S17. UV-visible absorption spectra for **1** as a function of H$^+$ concentration in [a] water; [b] 1:1 (*v/v*) water/methanol; [c] methanol.
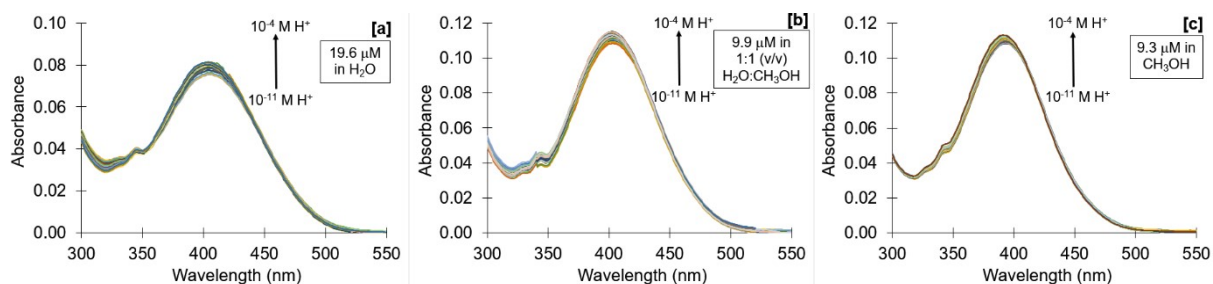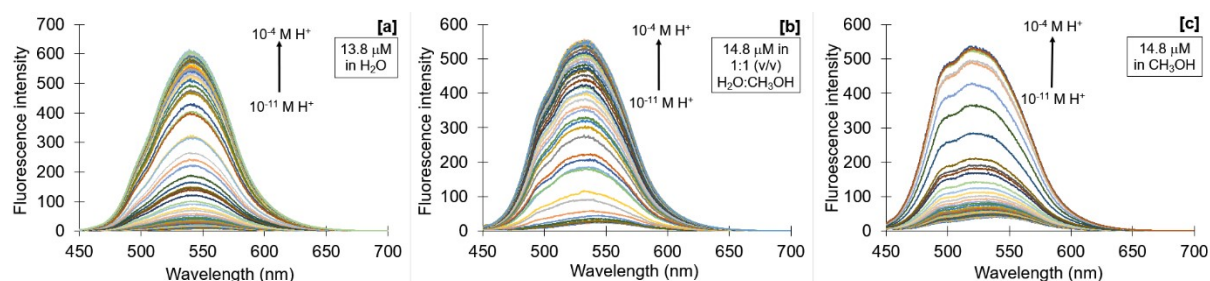

Figure S18. UV-visible absorption spectra for **2** as a function of H$^+$ concentration in [a] water; [b] 1:1 (*v/v*) water/methanol; [c] methanol.
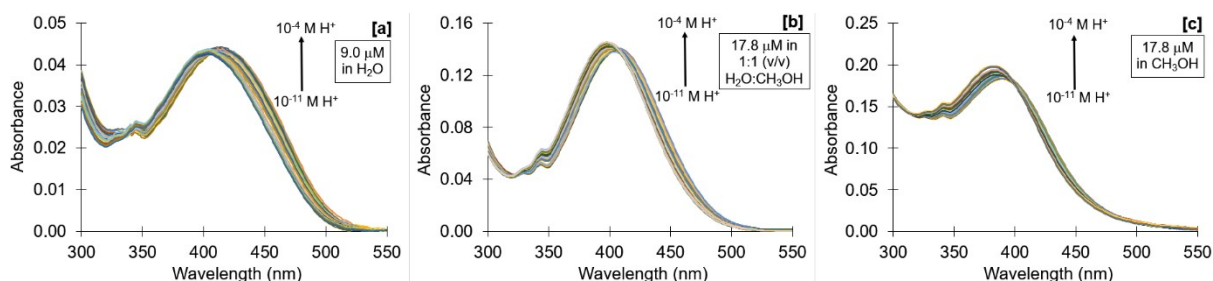
Figure S19. UV-visible absorption spectra for **3** as a function of H$^+$ concentration in [a] water; [b] 1:1 (*v/v*) water/methanol; [c] methanol.
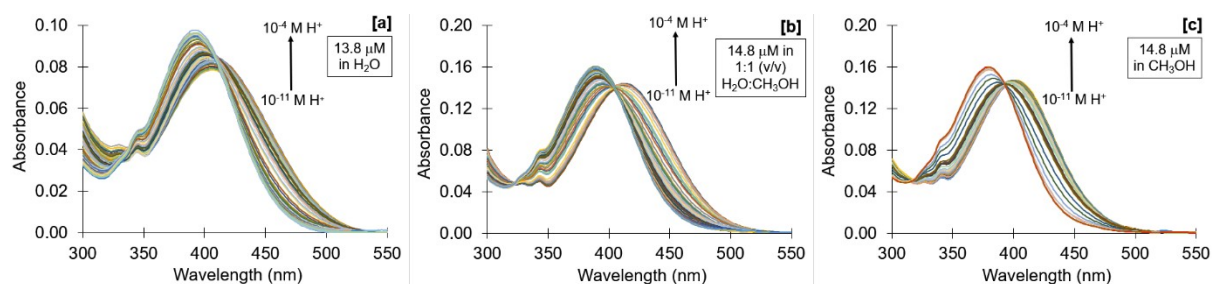
Figure S20. UV-visible absorption spectra for **4** as a function of H$^+$ concentration in [a] water; [b] 1:1 (*v/v*) water/methanol; [c] methanol.
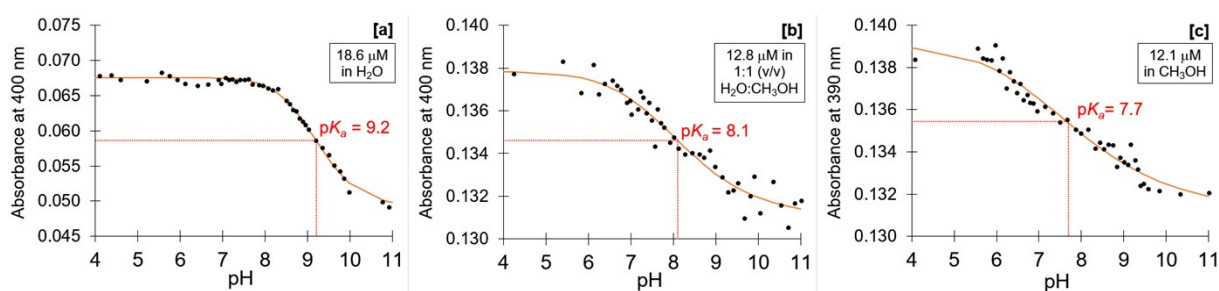
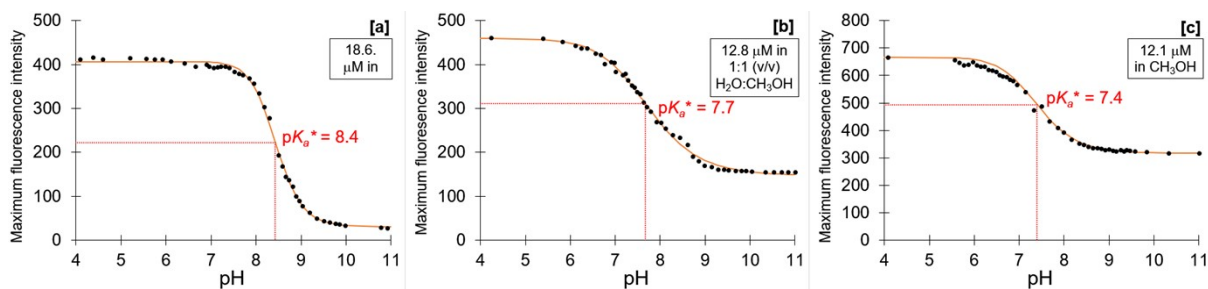**Figure S21.** Absorbance against pH graphs for **1** in [a] water; [b] 1:1 (*v/v*) water/methanol; [c] methanol.
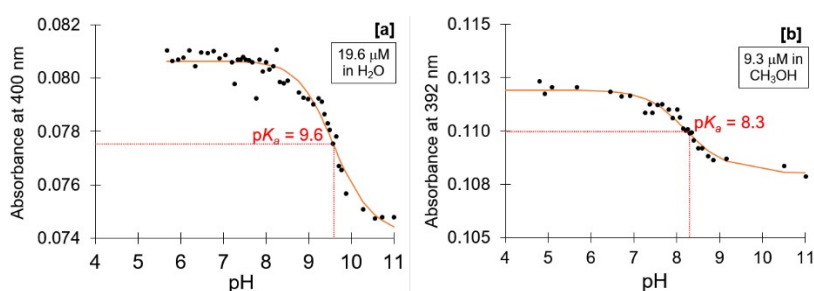
Figure S22. Absorbance against pH graphs for **2** in [a] water; [b] methanol.
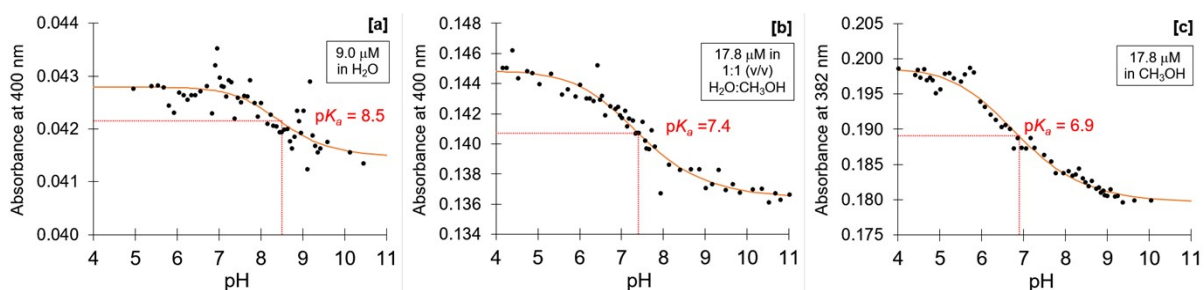
Figure S23. Absorbance against pH graphs for **3** in [a] water; [b] 1:1 (*v/v*) water/methanol; [c] methanol.
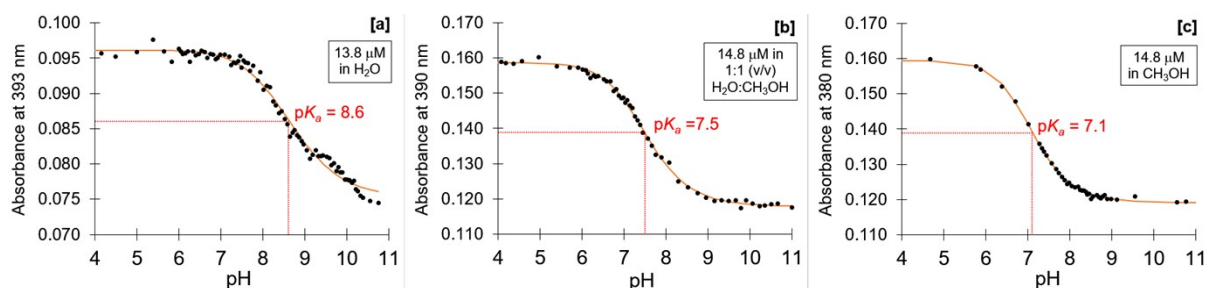
Figure S24. Absorbance against pH graphs for **4** in [a] water; [b] 1:1 (*v/v*) water/methanol; [c] methanol.
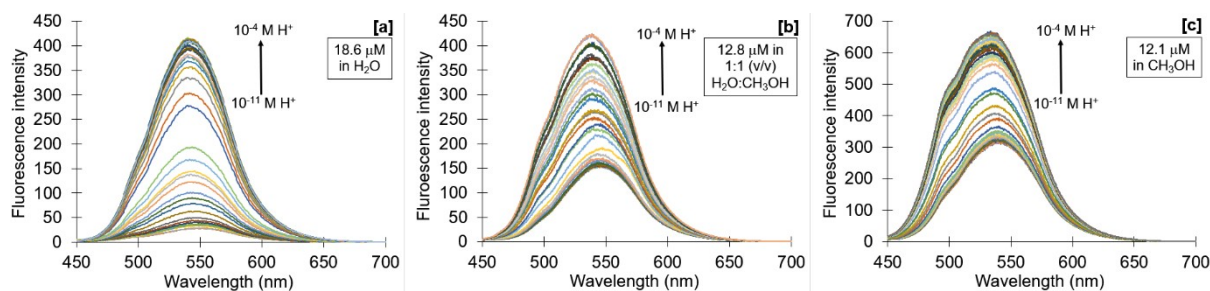
Figure S25. Fluorescence emission spectra for **1** as a function of H$^+$ concentration in [a] water; [b] 1:1 (*v/v*) water/methanol; [c] methanol. λ_{ex} = 400 nm.
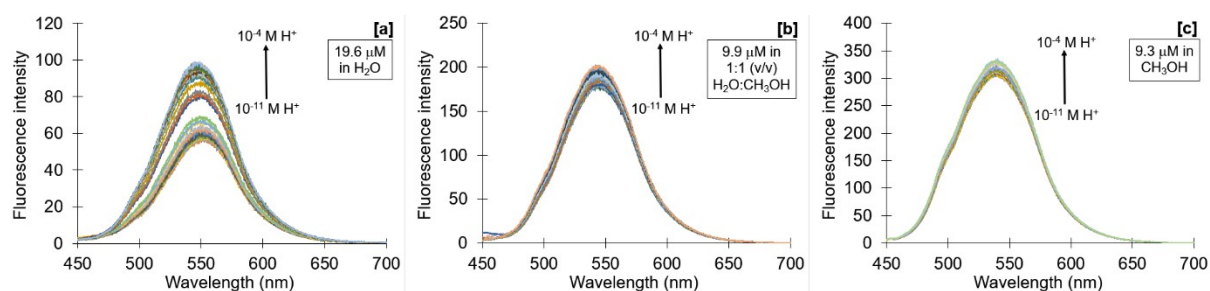
Figure S26. Fluorescence emission spectra for **2** as a function of H$^+$ concentration in [a] water; [b] 1:1 (*v/v*) water/methanol; [c] methanol. λ_{ex} = 400 nm.

Figure S27. Fluorescence emission spectra for **3** as a function of H$^+$ concentration in [a] water; [b] 1:1 (*v/v*) water/methanol; [c] methanol. λ_{ex} = 400 nm.

Figure S28. Fluorescence emission spectra for **4** as a function of H$^+$ concentration in [a] water; [b] 1:1 (*v/v*) water/methanol; [c] methanol. λ_{ex} = 400 nm.
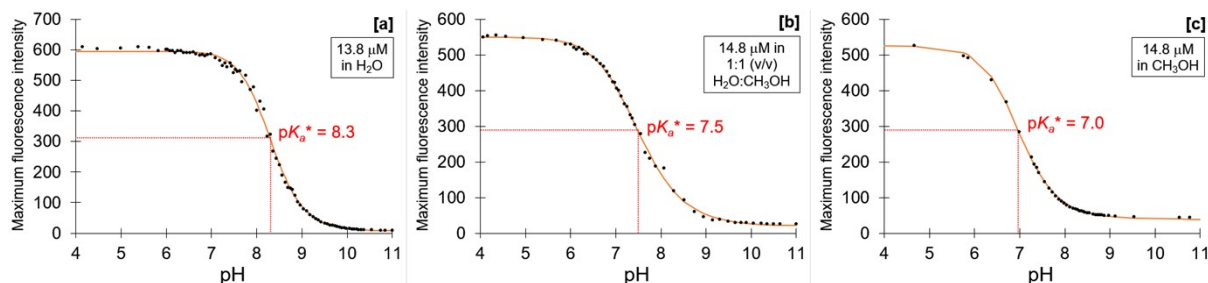
Figure S29. Maximum fluorescence intensity against pH graphs for **1** in [a] water; [b] 1:1 (*v/v*) water/methanol; [c] methanol. λ_{ex} = 400 nm.
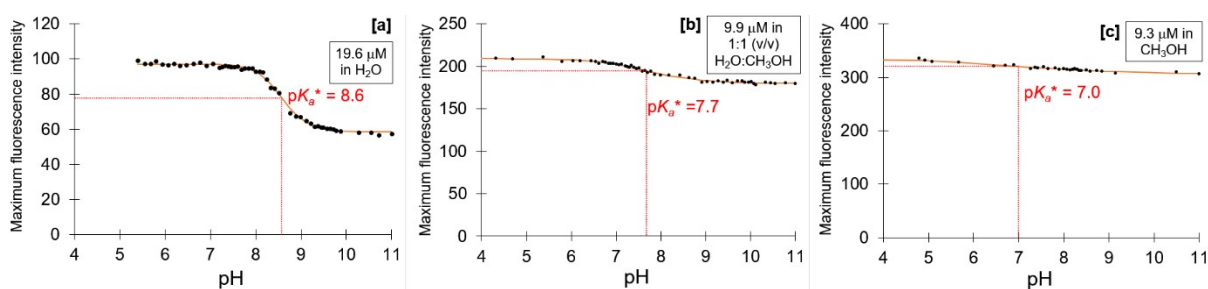
Figure S30. Maximum fluorescence intensity against pH graphs for **2** in [a] water; [b] 1:1 (*v/v*) water/methanol; [c] methanol. λ_{ex} = 400 nm.
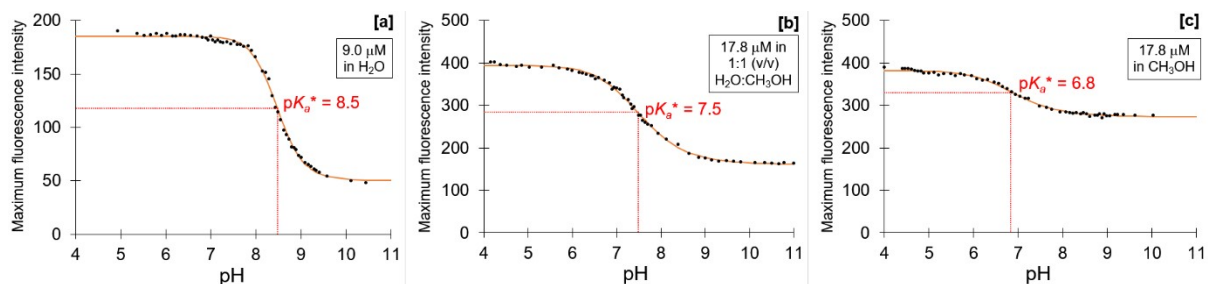
Figure S31. Maximum fluorescence intensity against pH graphs for **3** in [a] water; [b] 1:1 (*v/v*) water/methanol; [c] methanol. λ_{ex} = 400 nm.

Figure S32. Maximum fluorescence intensity against pH graphs for **4** in [a] water; [b] 1:1 (*v/v*) water/methanol; [c] methanol. λ_{ex} = 400 nm.

3.2. Cation UV-vis absorption and emission spectra for 3 and 4
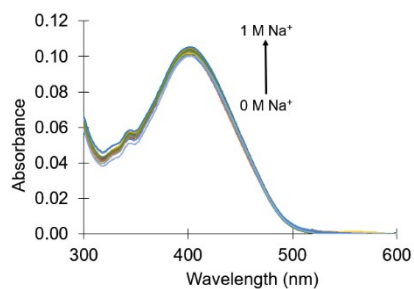
Figure S33. UV-visible absorption spectra for 10.6 μM **3** as a function of Na^+ concentration in 1:1 (*v/v*) water/methanol.
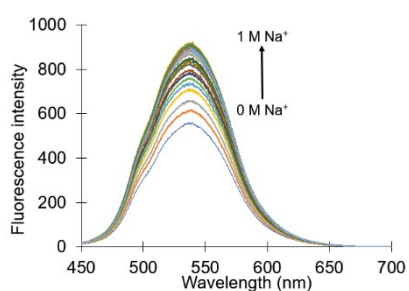
Figure S34. Fluorescence emission spectra for 10.6 μM **3** as a function of Na^+ concentration in 1:1 (*v/v*) water/methanol. λ_{ex} = 400 nm.
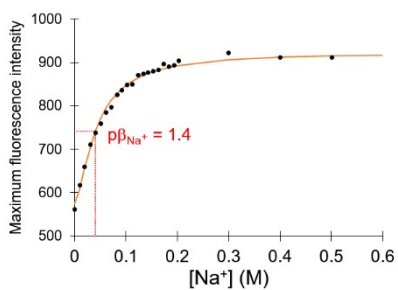

Figure S35. Maximum fluorescence intensity against Na^+ concentration graph for 10.6 μM **3** in 1:1 (*v/v*) water/methanol. λ_{ex} = 400 nm.
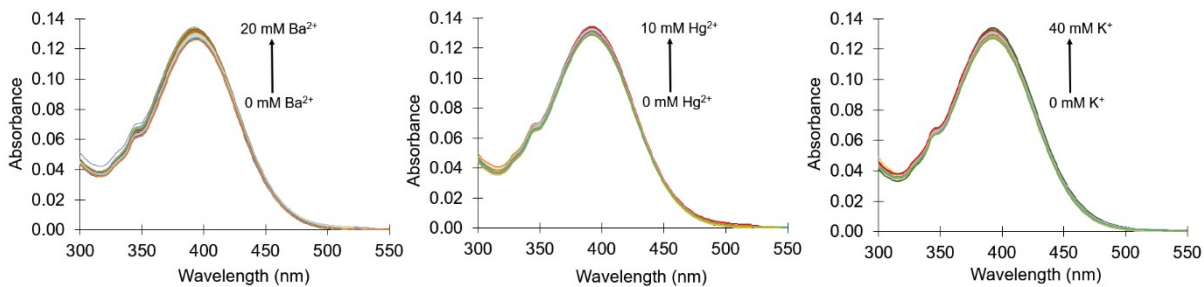
Figure S36. UV-visible absorption spectra for 14 μM **4** as a function of Ba^{2+}, Hg^{2+}, and K^+ concentration in water.
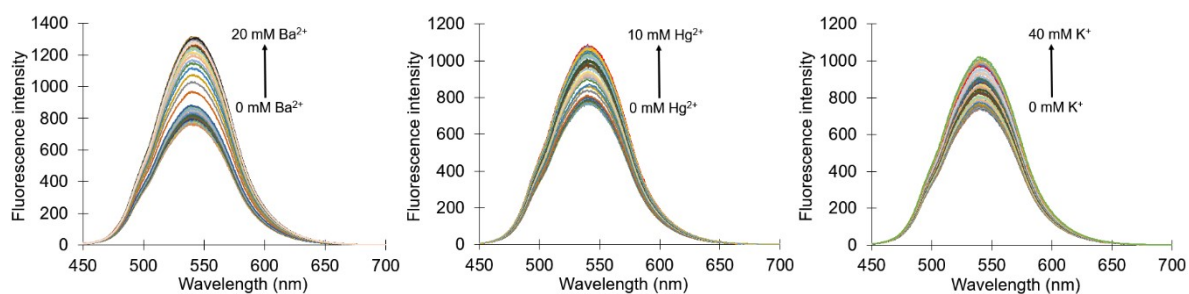

Figure S37. Fluorescence emission spectra for 14 μM **4** as a function of Ba^{2+}, Hg^{2+}, and K^+ concentration in water. $\lambda_{ex} = 400$ nm.
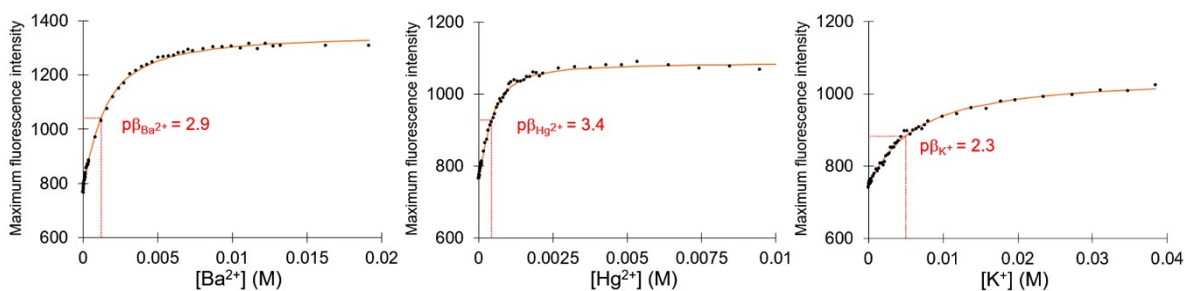

Figure S38. Maximum fluorescence intensity against cation concentration for 14 μM **4** as a function of Ba^{2+}, Hg^{2+}, and K^+ concentration in water. $\lambda_{ex} = 400$ nm.
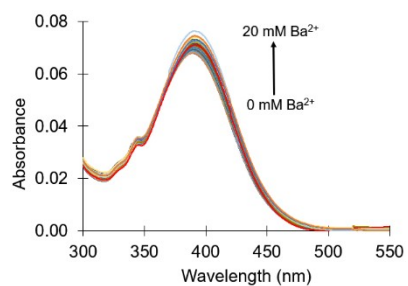
Figure S39. UV-visible absorption spectra for 7 μM **4** as a function of Ba^{2+} concentration in 1:1 (*v/v*) water/methanol.
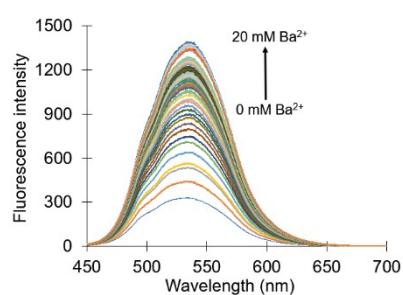

Figure S40. Fluorescence emission spectra for 7 μM **4** as a function of Ba^{2+} in 1:1 (*v/v*) water/methanol. $\lambda_{ex} = 400$ nm.
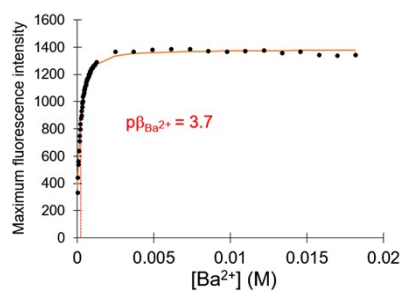

Figure S41. Maximum fluorescence intensity against Ba^{2+} concentration for 7 μM **4** in 1:1 (*v/v*) water/methanol. $\lambda_{ex} = 400$ nm.
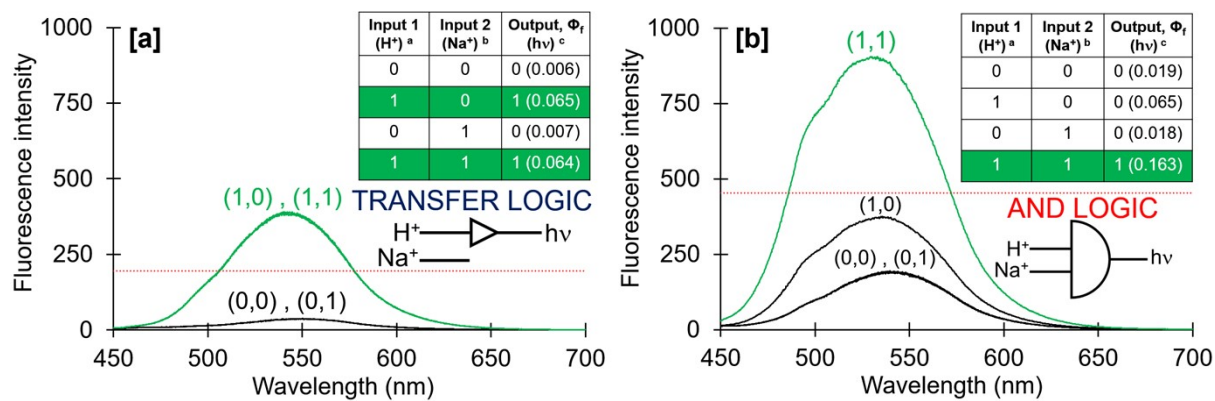
Figure S42. Fluorescence emission spectra of 9 μM **3** in (a) water and (b) methanol. The red line denotes the digital threshold, which was set at $\Phi_{fFmax}/2$. [a] Low input: 10^{-11} M H^+, high input: 10^{-4} M H^+; [b] low input: 0 mM Na^+, high input: 9 mM Na^+; [c] Measured with reference to quinine hemisulfate in 0.1 M H_2SO_4.

3.3. Spectroscopic data for 1-4

Table S1. Spectroscopic parameters of **1-4** in water, 1:1 (*v/v*) water/methanol, and methanol.

Parameter	Water ($\phi_{H_2O} = 1.0$)				1:1 (*v/v*) water/methanol ($\phi_{H_2O} = 0.5$)				Methanol ($\phi_{H_2O} = 0.0$)			
	1	**2**	**3**	**4**	**1**	**2**	**3**	**4**	**1**	**2**	**3**	**4**
$\lambda_{abs,\ 10^{-4}\,MH^+}$ (nm)	398	404	403	392	401	403	397	389	390	391	383	380
$\lambda_{abs,\ 10^{-11}\,MH^+}$ (nm)	406	405	417	406	403	403	407	413	393	393	389	401
$\varepsilon_{10^{-4}\,MH^+}$ (M^{-1} cm^{-1})	1660	3772	4695	3110	10951	11605	8306	10838	11580	12230	8698	11266
$\varepsilon_{10^{-11}\,MH^+}$ (M^{-1} cm^{-1})	1361	3190	3592	2398	8972	10545	7347	8655	10294	11114	8259	9430
$\lambda_{em,\ 10^{-4}\,MH^+}$ (nm) [a]	542	549	540	540	538	544	537	536	534	540	539	520
$\lambda_{em,\ 10^{-11}\,MH^+}$ (nm) [a]	549	551	554	556	546	547	549	546	540	540	540	540
$\Delta\lambda_{10^{-4}\,MH^+}$ (nm) [b]	144	145	137	148	137	141	140	147	144	149	156	140
$\Delta\lambda_{10^{-11}\,MH^+}$ (nm) [b]	143	146	137	150	143	144	142	133	147	147	151	139
λ_{isos} (nm)	345, 440	347, 455	338, 416	336, 409	420	424	322, 409	321, 405	413	420	313, 402	315, 394
$\Phi_{F,\ 10^{-4}\,MH^+}$ [c]	0.064	0.011	0.061	0.066	0.081	0.022	0.064	0.050	0.115	0.033	0.065	0.036
$\Phi_{F,\ 10^{-11}\,MH^+}$ [c]	0.006	0.008	0.009	0.002	0.010	0.019	0.014	0.002	0.019	0.031	0.019	0.002
FE [d]	15	1.7	4.2	72	3.0	1.2	2.5	22	2.1	1.1	1.4	13

| pK_a [e] | 9.2 | 9.6 | 8.5 | 8.6 | 8.1 | NA | 7.4 | 7.5 | 7.7 | 8.3 | 6.9 | 7.1 |
| pK_a* [f] | 8.4 | 8.6 | 8.5 | 8.3 | 7.7 | 7.7 | 7.5 | 7.5 | 7.4 | 7.0 | 6.8 | 7.0 |

[a] λ_{ex} = 400 nm. [b] $\Delta\lambda = \lambda_{em} - \lambda_{abs}$. [c] Measured with reference to quinine hemisulfate in 0.1 M H_2SO_4 [d] Proton-induced fluorescence enhancement, $I_{F_{10^{-4} M H^+}} / I_{F_{10^{-11} M H^+}}$. [e] Ground state measurements using eqn. 2. [f] Excited state measurements using eqn. 3.

4. NMR solvent studies for 3 and 4
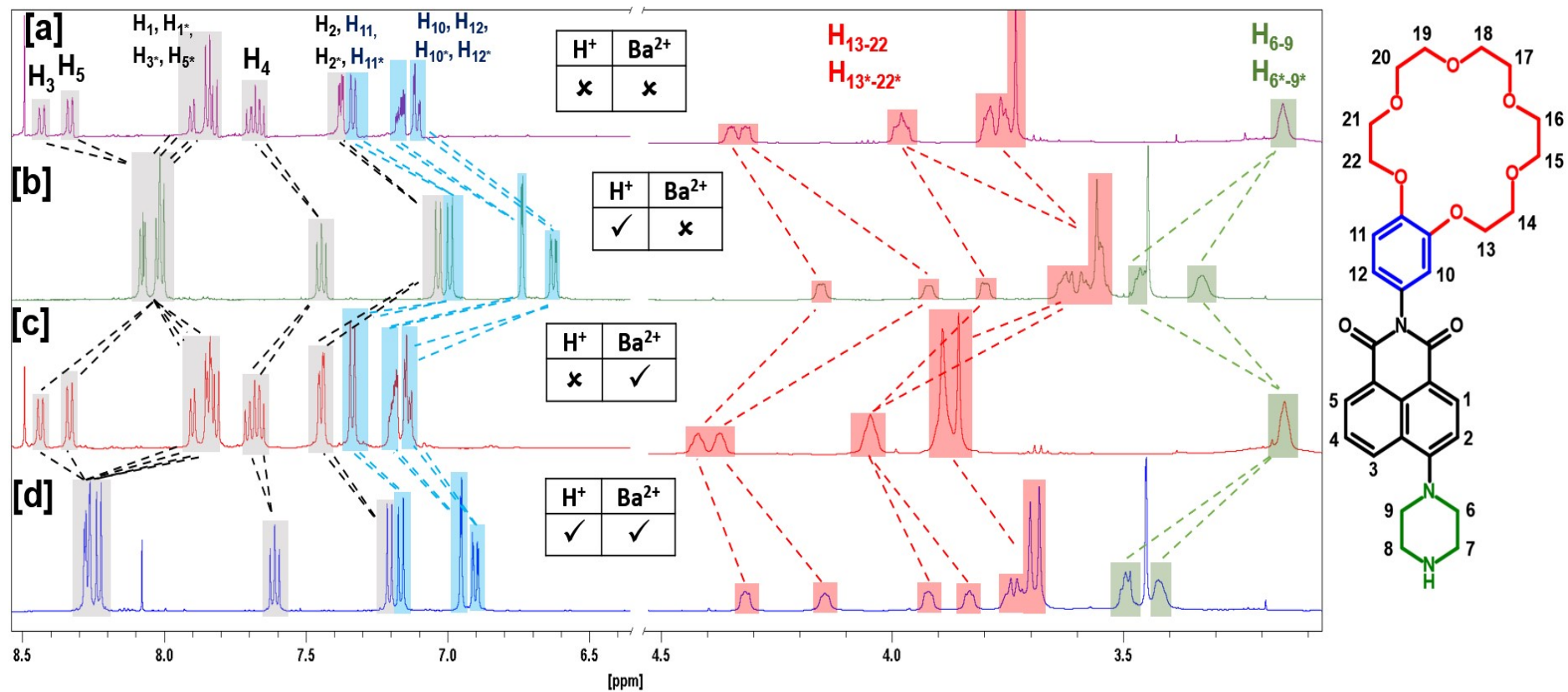
Figure S43. ^{1}H NMR spectra of 8 mM **4** in D_2O: (a) 50 mM NaOD added, (b) 50 mM DCl added, (c) 50 mM NaOD and 80 mM Ba^{2+}, (d) 50 mM DCl and 80 mM Ba^{2+}.
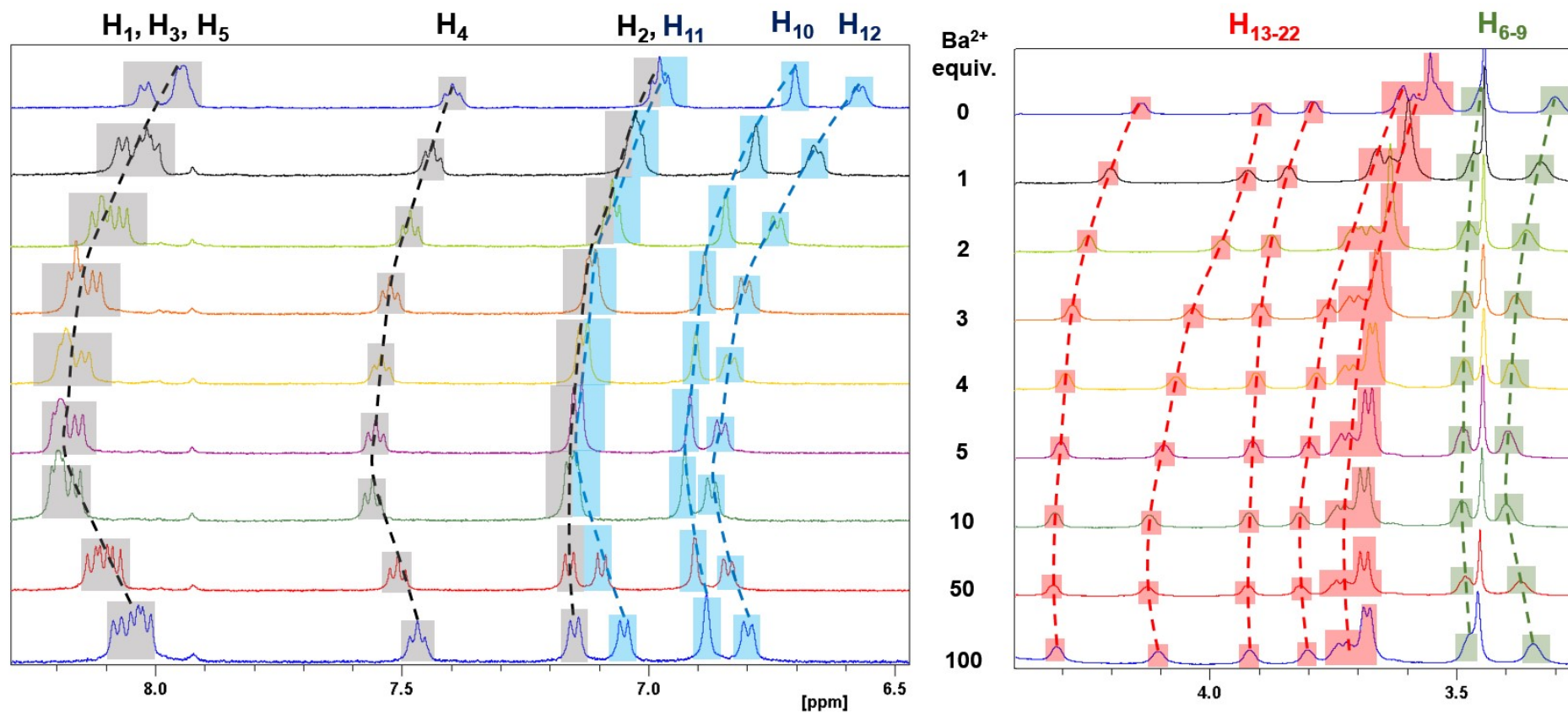
Figure S44. ^{1}H NMR data for 8 mM **4** in 10^{-4} M H$^+$ and 0-100 equivalents (0-800 mM) Ba^{2+} in D$_2$O.
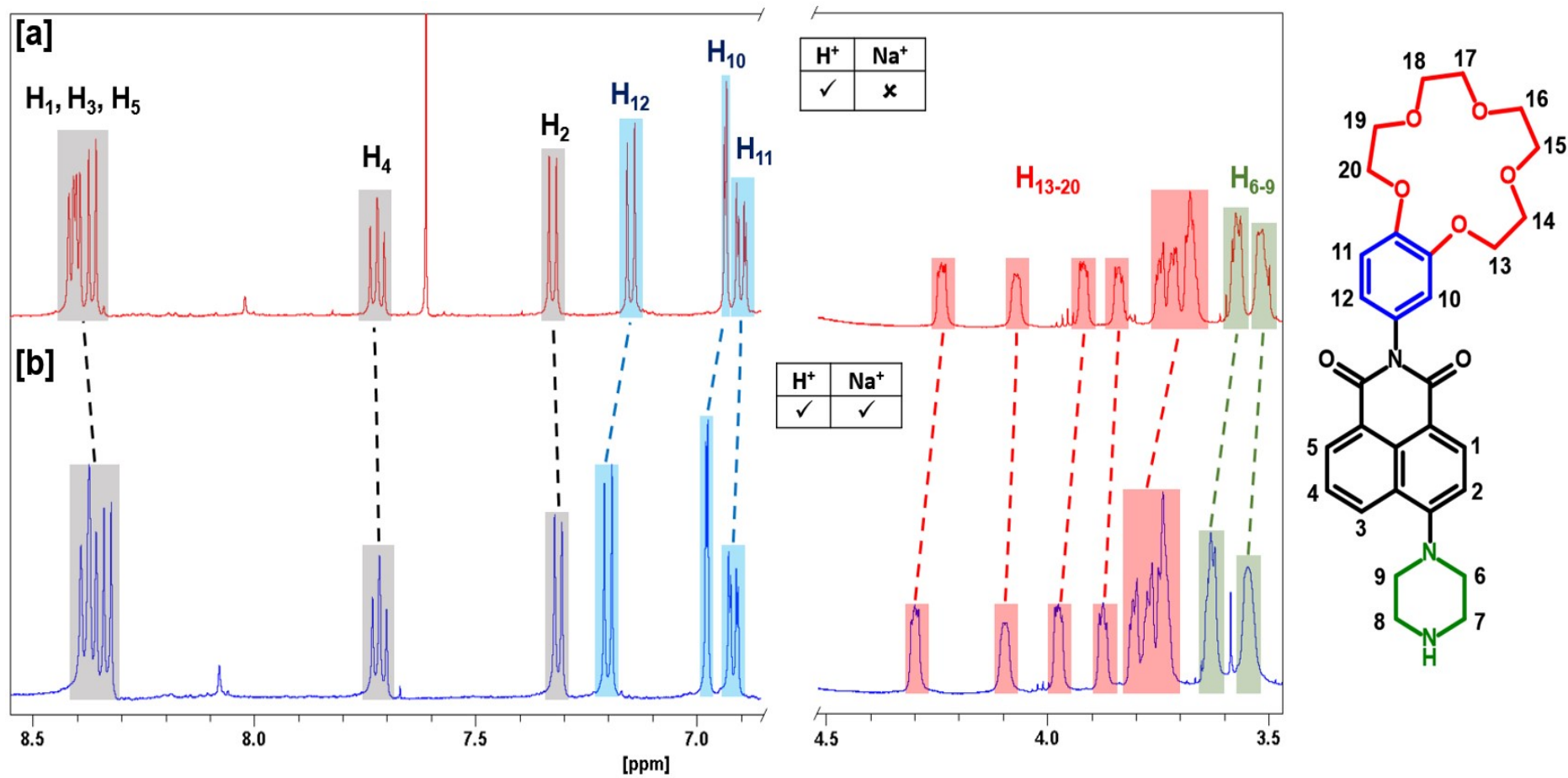
Figure S45: ^{1}H NMR spectra of 12 mM **3** in D_2O in [a] 10^{-4} M H^+; [b] 10^{-4} M H^+ and 120 mM Na^+ (10 equivalents).
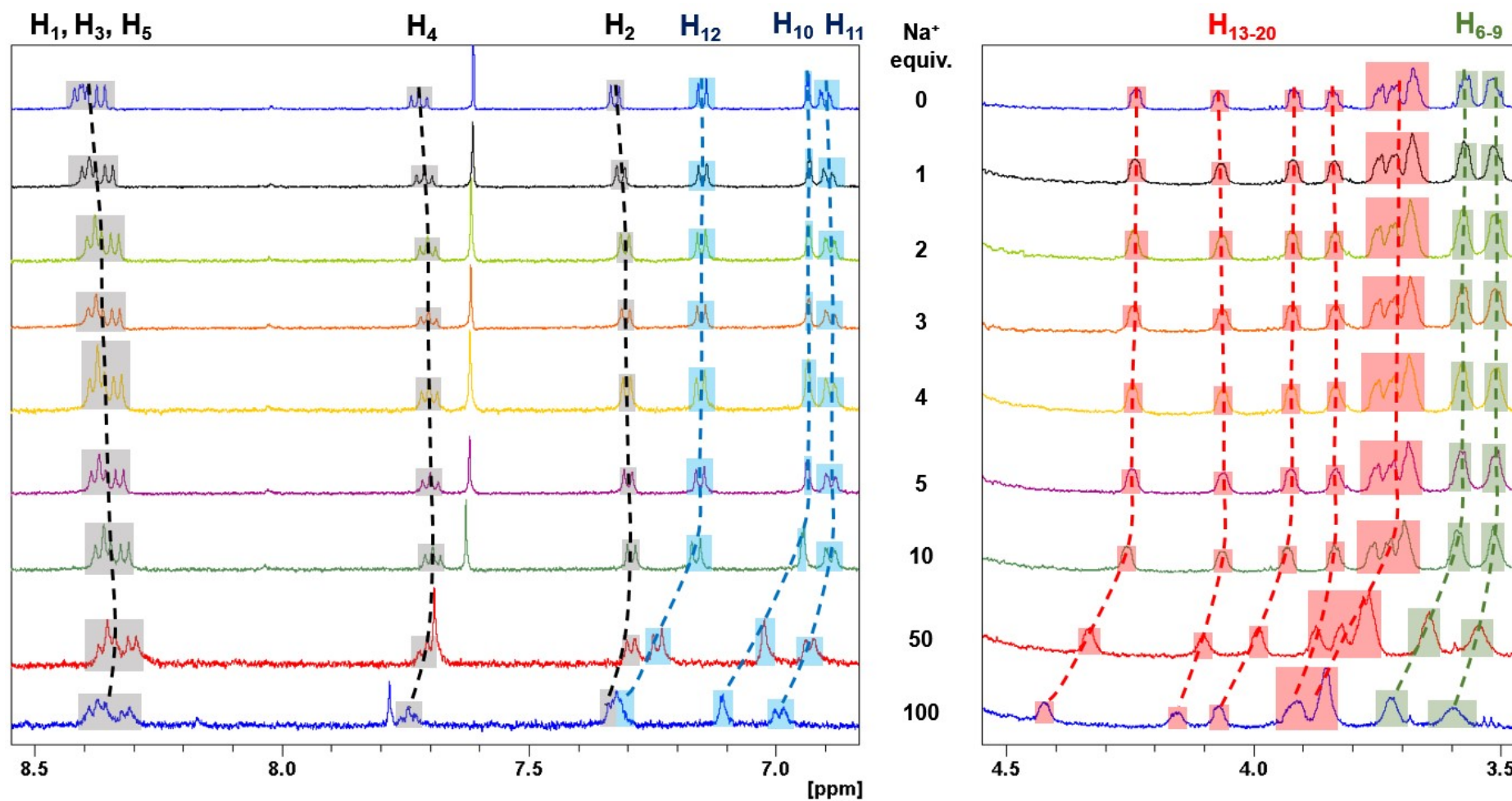
Figure S46: ¹H NMR spectra of **3**-H⁺ in D_2O with varying Na⁺ equivalents (0 to 100 equivalents; 0 M to 1.2 M).
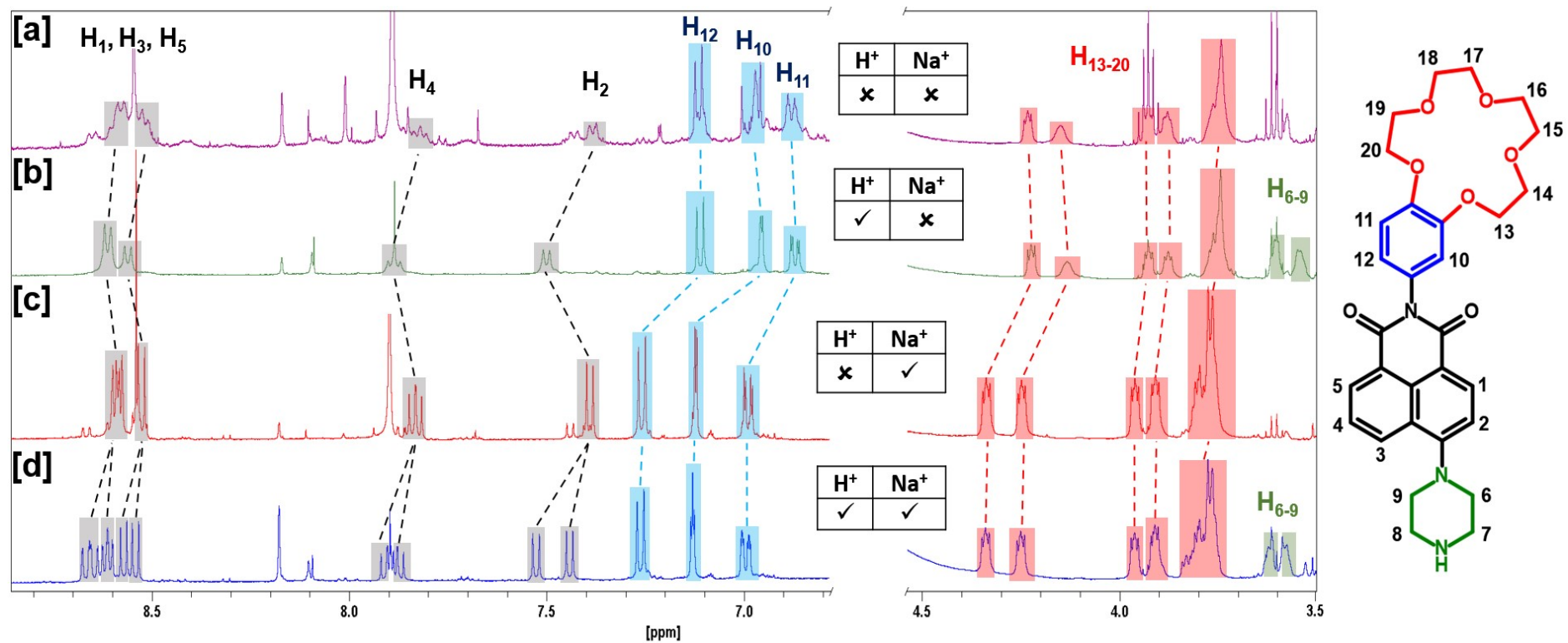
Figure S47: ^{1}H NMR spectra of 12 mM **3** in CD$_3$OD in [a] 10^{-11} M H$^+$; [b] 10^{-4} M H$^+$; [c] 10^{-11} M H$^+$ and 120 mM Na$^+$ (10 equivalents); [d] 10^{-4} M H and 120 mM Na$^+$ (10 equivalent).